Statistical Analysis

Experimental data were reported as the mean±standard deviation (s.d.). Group comparisons were made by Mann–Whitney tests, where appropriate, with Prism software (GraphPad Software, La Jolla, CA). Error bars indicate mean±s.d. A p-value of <0.05 was considered significant.

Results

CGD Patients Developed ILD with Increasing Serum Levels of KL-6

Among 33 patients with X-CGD who were followed at our hospital during the last 10 years, four (12 %) developed ILD during prophylactic treatment, as shown in Table 1. Two patients (Cases 1 and 3) showed mild restrictive ventilatory impairments by respiratory function testing (Table 1). As with other types of ILD, the serum levels of KL-6, thought to be a sensitive marker for ILD [11], increased to 1,030–4,000 IU/ml for these four patients at the onset of ILD. Conversely, serum levels of KL-6 were in the normal range (<500 IU/ml) for CGD patients without ILD (311±106 IU/ml; Fig. 1a and b). Although no pathogenic microorganisms were isolated from their blood and sputum cultures, and *Pneumocystis jirovecii* and *Mycobacterium* spp. were not detected by PCR assay using their sputa at the onset of ILD, it is difficult to completely deny the impact of infection on ILD. Accordingly, prophylactic treatment with itraconazole and trimethoprim/sulfamethoxazole was required in the ILD patients. Antibiotics and antifungal drugs did not have any therapeutic effects on ILD symptoms. One patient (Case 4) received periodical subcutaneous injections of IFNγ along with the prophylactic drugs (Table 1). The other three patients with ILD did not receive IFNγ and just one (Case 4) of ten CGD patients who had been treated with this therapy developed ILD (odds ratio=0.74), suggesting that IFNγ was unlikely to have been involved in the development of ILD.

Clinical Courses of CGD Patients with ILD

Case 1: The patient was a 20-year-old Japanese man who had been treated with 7.5 mg/day of corticosteroid for CGD-associated bowel inflammation. Just after working at a fruit-processing plant, he developed a cough which became persistent at 8 weeks. He subsequently quit this job to avoid breathing in the dust at the plant where he worked. Leaving the job improved his clinical symptoms and increased his oxygen saturation from 90 to 98 %. However, lung CT images still showed diffuse ground-glass opacity (Fig. 2a) and serum KL-6 levels remained high (Fig. 1b). An oral corticosteroid was increased to 40 mg/day at 12 weeks after the onset of ILD. Although the increased corticosteroid resulted in some improvements of ILD on CT images, this therapy worsened his pulmonary fungus infection. Thus, the dose of this drug was reduced and thalidomide therapy was started at 38 weeks after the onset of ILD. Subsequently, his clinical condition, including CT findings, was relatively stable and his serum KL-6 levels gradually decreased with corticosteroid and thalidomide therapy (Fig. 1b).

Case 2: The patient was an 8-year-old Japanese boy. ILD was serendipitously identified by CT images acquired for follow-up of lung abscesses he had since 4 years old (Fig. 2b). As the nodular consolidation of CT images did not improve after more than one antibiotic or antifungal drug use, he was treated with 0.5 mg/kg/day of a corticosteroid at 8 weeks after the onset of ILD. His serum KL-6 levels declined after this therapy (Fig. 1b), but increased again with gradual tapering of the corticosteroid dose.

Table 1 Characteristics of the CGD patients with ILD

Case	Age at diagnosis of ILD (year-old)	Prophylactic treatment			Respiratory signs and symptoms			Lung function	
		IFNγ (JRU/m^2/week)	Trimethoprim / Sulfamethoxazole (g/kg/day)	Itraconazole (mg/kg/day)	Crackle	Cough	Fever	FEV1.0%[a]	%VC[b]
1	20	–	0.07	4.4	+/–	+	+	86.2	72.5
2	8	–	0.06	5.0	–	–	–	81.1	103.4
3	23	–	0.08	4.0	–	+	+	73.1	72.8
4	8	25×10^4	0.06	5.0	–	–	–	93	75.6

[a] FEV1.0 %, forced expiratory volume 1.0 s %; Normal range >70

[b] 2 %VC, % vital capacity; Normal range >80

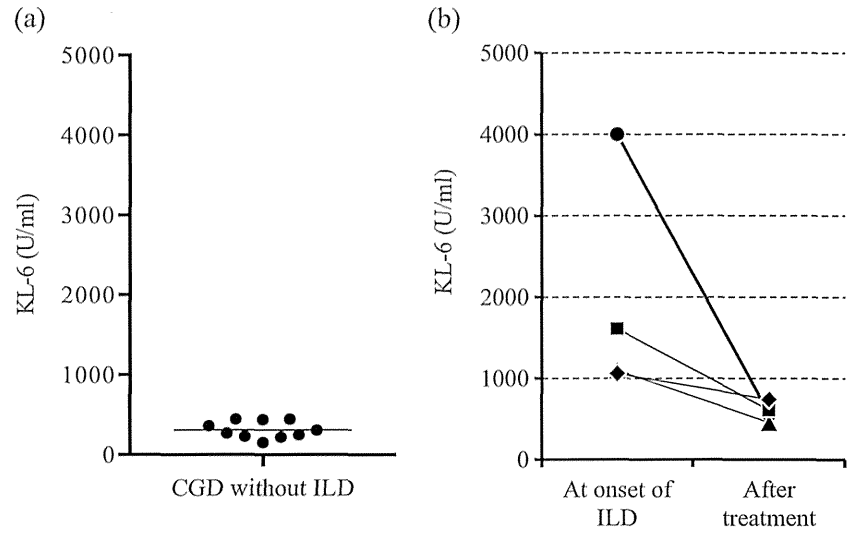

Fig. 1 Serum KL-6 levels of CGD patients with and without ILD. **a** Serum KL-6 levels were determined for CGD patients who previously had pulmonary infections caused by bacteria or fungi (311±106 IU/ml; $n=10$). **b** Serum KL-6 levels of Case 1 (*circles*), Case 2 (*triangles*), Case 3 (*squares*) and Case 4(*diamonds*) at the onset of ILD and after treatment

Case 3: The patient was a 23-year-old Japanese man. After moving to a new residence, he developed a persistent cough and a prolonged fever for 2 months despite the administration of antibiotics and antifungal drugs at our hospital. He had high KL-6 serum levels (Fig. 1b) and CT images showed diffuse ground-glass opacity at the onset of ILD (Fig. 2c). He moved back to his previous residence as an allergen avoidance measure. This resulted in a decline of his serum KL-6 levels and improvements on CT images without any medications (Fig. 1b).

Case 4: The patient was an 8-year-old Japanese boy who received periodical subcutaneous injections of IFNγ together with prophylactic drugs (Table 1). He was scheduled to receive thalidomide therapy for CGD colitis. A pulmonary CT scan taken as a screening test before thalidomide therapy revealed an ILD lesion (Fig. 2d) and an elevated serum KL-6 level (Fig. 1b). Thalidomide therapy resulted in a decline of his serum KL-6 levels; however, the levels increased again upon discontinuation of therapy (Fig. 1b).

Pathological Findings for ILD Patients Revealed Inflammation of Interstitial Lung Tissue

To assess the pathological changes in the lung lesions of the ILD patients, we collected BALF by bronchoscopy for Cases

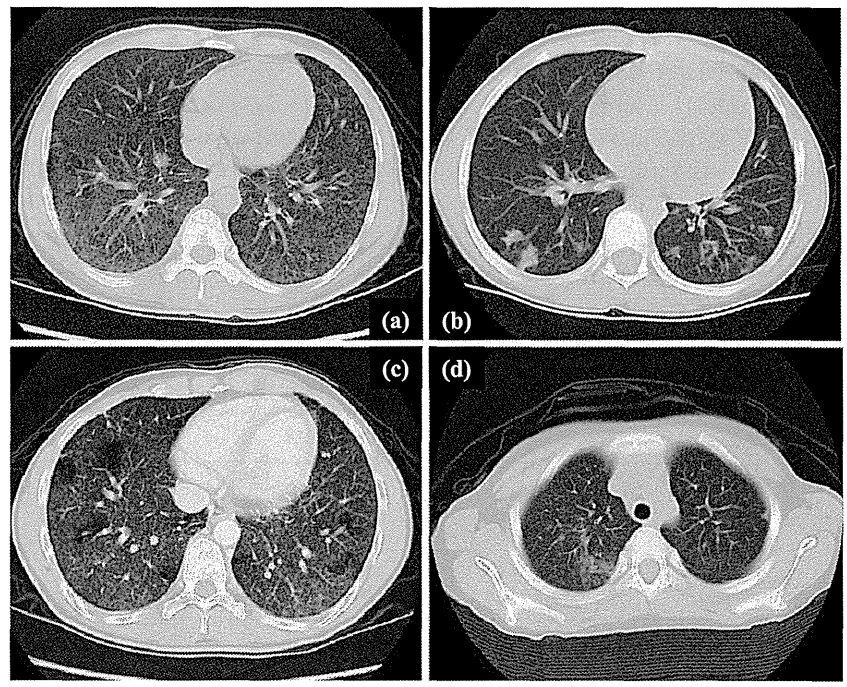

Fig. 2 Computed tomographic lung images at the onset of ILD. Representative chest CT images revealed ground glass opacity for Case 1 (**a**), Case 2(**c**), Case 3(**c**) and Case 4 (**d**), and nodular consolidation for Case 2 (**b**) at the onset of ILD

1, 2, and 3. Although the number of cells in BALF varied among these cases, the main fractions were lymphocytes. Conversely, in CGD patients with pulmonary aspergillosis, the fractions were predominantly macrophages (n=3 for CGD patients with aspergillosis, Table 2). Flow cytometry analyses revealed that most lymphocytes in BALF were $CD3^+$ T cells, and the ratio of $CD4^+$ to $CD8^+$ T cells was less than 1.0 for Cases 1 and 3, which suggested that most lymphocytes were $CD3^+CD8^+$ cytotoxic T cells in these patients with diffuse pulmonary lesions (Table 2).

Lung tissue samples were obtained from Cases 1 and 3 by surgical lung biopsy and examined after hematoxylin and eosin staining to assess pathological changes in these lesions. Homogeneous microgranuloma formation surrounded by the infiltration of multi-nucleated giant cells and lymphocytes were revealed, which was reminiscent of those seen with HP (Fig. 3a and b). Since blood and lymphatic vessels were not occupied by granulomas, and that proteinase three anti-neutrophil cytoplasmic antibodies (PR-3ANCA) in serum were negative for these cases, the likelihood of sarcoidosis and Wegener's granulomatosis was low. As well, no pathogenic microorganisms were isolated from BALF and lung tissues.

High Levels of Specific IgG to *Aspergillus fumigatus* in Serum of CGD Patients

Pulmonary aspergillosis can be distinguished into two types; infection and hypersensitivity respiratory disorders including HP that is caused by a prototypical type-III and type-IV allergic inflammatory reaction [15]. In order to assess the exposure to *Aspergillus* spp. in CGD patients, we determined serum levels of specific IgG antibodies against *A. fumigatus*, a common genus in living environment. The concentration of specific IgG to *A. fumigatus* in the serum of CGD patients was significantly higher than that of healthy subjects, while there was no difference between CGD patients with and without ILD (108.3±7.5 U/ml, 143.4±64.3 U/ml and 12.5±16.6 U/ml for CGD patients with and without ILD and healthy subjects, respectively, Fig. 4).

Infiltrating Cells in ILD Patients' Pulmonary Lesions were Activated and Produce Large Amounts of Inflammatory Cytokines

To assess whether inflammatory cytokines, including IL-6, IL-8, TNFα, and IFNγ, were involved in the pathogenic changes in ILD pulmonary lesions, we measured these cytokines in BALF samples. Interestingly, the levels of these cytokines in BALF samples from ILD patients were much higher than those of CGD patients with pulmonary aspergillosis (Fig. 5a). By comparison, the serum levels of these cytokines for ILD patients fell between those of CGD patients without demonstrable infections and healthy subjects (Fig. 5b). This suggested that in ILD patients, PBMCs were not activated in the peripheral blood but in the pulmonary lesions instead (Fig. 5b). This was also confirmed by an in vitro cytokine production assay whereby the amounts of these inflammatory cytokines produced by PBMCs and cells obtained from BALF were measured.

There were no differences in the serum levels of the inflammatory cytokines between ILD patients and CGD patients without demonstrable infections. Hence, circulating PBMCs should have been similarly activated in both of these groups. When cultured under conditions of no stimulation, cells obtained from BALF samples for Cases 1 and 2 produced higher amounts of these cytokines than the unstimulated PBMCs from CGD patients (Fig. 6). This suggested that only infiltrating cells in the pulmonary lesions were activated and produced large amounts of inflammatory cytokines in ILD patients.

Discussion

Since CGD patients have susceptibility to infection, some residual pathogens may have persisted and invaded their lungs partially. In our cases, the initial symptoms of ILD might overlap with residual pathogen and microgranuloma formation due to hyperinflammation; however, increased levels of

Table 2 Assessments of ILD patients' bronchoalveolar lavage fluids

	Cellularity (10^5 cells/ml)	Cell differentiation (%)				Lymphocyte (%)			CD4/CD8
		Macrophage	Lymphocyte	Eosinophil	Neutrophil	CD3	CD4	CD8	
Case 1	10.1	34	66	0	0	98	39.9	47.2	0.8
Case 2	3.2	24	75.5	0.5	0	82	57.4	24.4	2.4
Case 3	19	23.8	73.4	0.2	2.2	98.9	40.6	56.4	0.7
Aspergillosis	5.3±6.3	78.2±11.1	20.2±9.7	0.3±0.6	1.3±1.2	89.9±4.4	63.3±11.1	26.1±5.1	2.5±0.9
Normal range	0.2–1.0	75–95	4.0–25	<1.0	–	–	33–57	14–28	1.5–3.2

Aspergillosis, CGD patients who suffer from pulmonary aspergillosis (n=3)

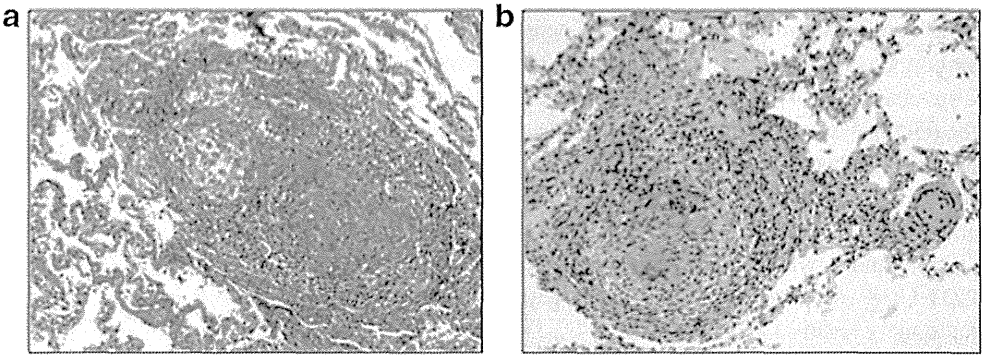

Fig. 3 Pathological findings reveal homogeneous microgranulomas formation in ILD patients' lungs. Pathologic evaluations showed infiltrations of inflammatory cells and homogeneous formations of microgranulomas on pulmonary sections stained with hematoxylin and eosin at the onset of ILD for Case 1 (**a**) and Case 3 (**b**)

serum KL-6 and failure of adequate therapy directed at bacterial and fungal infection could lead to consideration of other etiologies such as hyperinflammation in CGD. Meanwhile, there is a previous report of a CGD patient who developed interstitial inflammation of lung resulting from hyperinflammation associated with CGD [16].

HP is a pulmonary interstitial inflammatory disease caused by type-III and type-IV allergic inflammatory reaction to more than 300 inhalation allergens, including *Aspergillus* spp. [15, 17]. The specific IgG to *Aspergillus* was increased in serum of CGD patients, which was also observed in patients with HP [18]. Based on the disease duration, HP is categorized as acute, sub-acute, or chronic [19]. As there is no demonstrable evidence of progressive infection and the clinical course, including pathological findings, that are similar to those of HP, the mechanisms of ILD in these cases may be associated with HP. If so, the incidence of ILD is probably much higher in CGD patients because the frequency of HP is four per million children [20]. In our study, we identified four ILD patients out of 33 X-CGD patients (12 %). It is intriguing that there was a discrepancy between clinical phenotypes and pathological findings, in that the clinical courses of our ILD patients were reminiscent of sub-acute HP, whereas the pathological findings of homogeneous microgranulomas reflected typical acute HP.

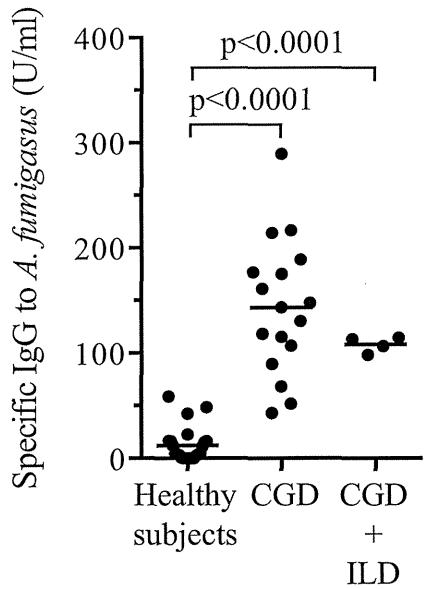

Fig. 4 Specific IgG antibody to *Aspergillus fumigatus* in CGD patients with and without ILD. Specific IgG antibody to *Aspergillus fumigatus* in serum was increased in CGD patients with and without ILD compared to that of healthy subjects

The involvement of IFNγ therapy with the development of ILD cannot be ruled out completely. However, because three of our patients who did not receive IFNγ therapy developed ILD, this may undermine the possibility. In particular, the clinical symptoms in two patients (Cases 1 and 3) were mitigated only by allergen avoidance, proving that CGD patients were more susceptible to ILD triggered by prolonged hyperinflammation resulting from inhalation antigens.

Recently, the clinical symptoms of auto-inflammation, such as granuloma formation or CGD colitis, were reported in CGD [7, 4]. A plausible explanation is that a deficit of ROS generation due to impaired NOX function in CGD patients prolongs NF-κB activation and caspsase-1 deactivation, which results in hyperinflammation [6]. This is because ROS are negative regulators for inflammatory cytokine production through the ERK, NF-κB, and caspsase-1 signaling pathway [8, 21]. In keeping with this, the PBMCs of CGD patients would be activated to produce inflammatory cytokines due to the effects of remaining pathogens, even in a static state [7]. Importantly, cells in BALF samples were activated to produce large amounts of inflammatory cytokines compared to the PBMCs of CGD patients, suggesting that the sites of inflammation were localized to the lungs due to inhalation of antigens. Previous reports of p47phox and gp91phox-deficient mice developing exaggerated progressive lung inflammation following inhalation of zymosan or LPS may provide a basis for our findings [22]. Zymosan is a fungal wall component that induces an innate immune response [23]. Elevated specific IgG antibody to *A. fumigatus* in CGD patients suggests that the patients are repeatedly exposed to an *Aspergillus* component which activates alveolar macrophages [24].

While avoidance of allergen exposure, such as relocating or changing jobs, is the initial therapy for HP, this measure alone

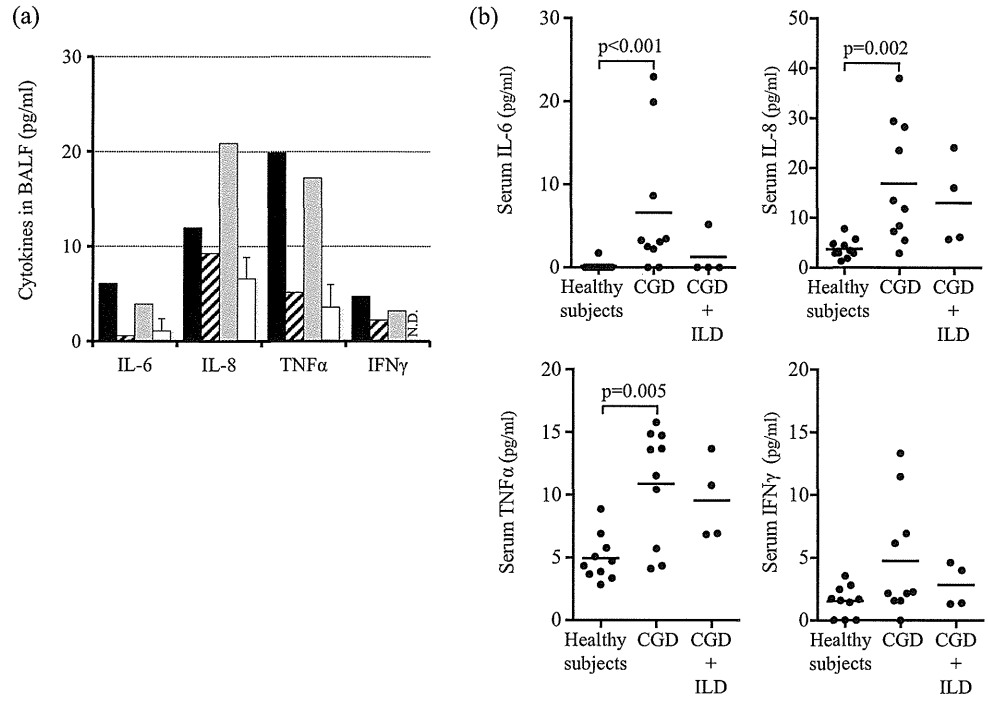

Fig. 5 Cytokine levels in bronchoalveolar lavage fluid and serum are increased in CGD patients. **a** BALF concentrations of IL-6, IL-8, TNFα, and IFNγ for Case 1 (*black bars*), Case 2 (*striped bars*), Case 3 (*gray bars*), and CGD patients who developed pulmonary aspergillosis (white bars, $n=3$). **b** Serum levels of IL-6, IL-8, TNFα, and IFNγ in ILD patients, CGD patients without demonstrable infection ($n=10$), and healthy subjects ($n=10$)

may be insufficient to provide ILD patients with complete therapeutic effects for their clinical symptoms, as their PBMCs lack negative regulators of ROS for inflammatory cytokine production. Meanwhile, anti-inflammatory therapy using steroid (e.g., oral corticosteroid) has been reported to be successful in controlling CGD colitis [25]. However, it should be noted that this therapy often increases a patient's susceptibility to infection [26], as was the situation in Case 1. From this perspective, thalidomide therapy should be considered for CGD patients with ILD because it potentially suppresses inflammation by decreasing inflammatory cytokine production through inhibition of NF-κB. This mode of action has been demonstrated in patients with Behcet's disease, rheumatoid arthritis, and Crohn's disease [27–30]. Also, thalidomide therapy exerts has a smaller negative effect on host defense [31]. Previously, we have reported that thalidomide attenuated excessive inflammation without increasing the susceptibility to infection in a patient with CGD colitis [7].

Conclusions

We described the clinical courses of 4 X-CGD patients with ILD and assessed the functions of PBMCs from CGD patients based on the cells' production of inflammatory cytokines. Although their pathological findings were reminiscent of HP,

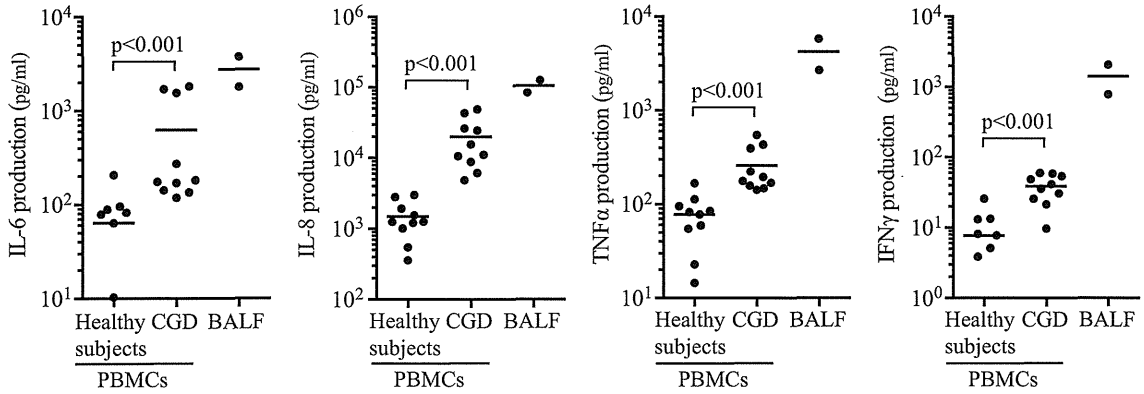

Fig. 6 Cytokine production by PBMCs and infiltrating cells in BALF. Cytokine levels were determined in culture supernatants after PBMCs or BALF cells were cultured for 16 h without stimulation. Concentrations of IL-6, IL-8, TNFα, and IFNγ in culture supernatants of infiltrating cells obtained from BALF and PBMCs obtained from CGD patients without demonstrable infection ($n=10$) and healthy subjects ($n=10$)

it was likely that ILD was caused by excessive inflammation resulting from an inadequate production of ROS in CGD. In addition to CGD-associated bowel inflammation, ILD with microgranulomas may also be one of the characteristic auto-inflammatory diseases for CGD patients.

Acknowledgments We are grateful to the CGD patients and blood donors for their participation in this study. The manuscript was proofread and edited by Dr. Julian Tang of the Department of Clinical Research Education, National Center for Child Health and Development. This study was supported by a Grant from the National Center for Child Health and Development.

Conflict of Interest The authors declare no competing financial interests.

References

1. Kang EM, Marciano BE, DeRavin S, Zarember KA, Holland SM, Malech HL. Chronic granulomatous disease: overview and hematopoietic stem cell transplantation. J Allergy Clin Immunol. 2011;127(6):1319–26.
2. Kawai T, Kusakabe H, Seki A, Kobayashi S, Onodera M. Osteomyelitis due to trimethoprim/sulfamethoxazole-resistant Edwardsiella tarda infection in a patient with X-linked chronic granulomatous disease. Infection. 2011;39(2):171–3.
3. Kobayashi S, Murayama S, Takanashi S, Takahashi K, Miyatsuka S, Fujita T, et al. Clinical features and prognoses of 23 patients with chronic granulomatous disease followed for 21 years by a single hospital in Japan. Eur J Pediatr. 2008;167(12):1389–94.
4. Holland SM. Chronic granulomatous disease. Clin Rev Allergy Immunol. 2010;38(1):3–10.
5. De Ravin SS, Naumann N, Cowen EW, Friend J, Hilligoss D, Marquesen M, et al. Chronic granulomatous disease as a risk factor for autoimmune disease. J Allergy Clin Immunol. 2008;122(6):1097–103.
6. van de Veerdonk FL, Smeekens SP, Joosten LA, Kullberg BJ, Dinarello CA, van der Meer JW, et al. Reactive oxygen species-independent activation of the IL-1beta inflammasome in cells from patients with chronic granulomatous disease. Proc Natl Acad Sci U S A. 2010;107(7):3030–3.
7. Kawai T, Watanabe N, Yokoyama M, Arai K, Oana S, Harayama S, et al. Thalidomide attenuates excessive inflammation without interrupting lipopolysaccharide-driven inflammatory cytokine production in chronic granulomatous disease. Clin Immunol. 2013;147(2):122–8.
8. Fernandez-Boyanapalli R, Frasch SC, Riches DW, Vandivier RW, Henson PM, Bratton DL. PPARgamma activation normalizes resolution of acute sterile inflammation in murine chronic granulomatous disease. Blood. 2010;116(22):4512–22.
9. Seger RA. Modern management of chronic granulomatous disease. Br J Haematol. 2008;140(3):255–66.
10. Uzel G, Orange JS, Poliak N, Marciano BE, Heller T, Holland SM. Complications of tumor necrosis factor-alpha blockade in chronic granulomatous disease-related colitis. Clin Infect Dis Off Publ Infect Dis Soc Am. 2010;51(12):1429–34.
11. Kohno N, Kyoizumi S, Awaya Y, Fukuhara H, Yamakido M, Akiyama M. New serum indicator of interstitial pneumonitis activity. Sialylated carbohydrate antigen KL-6. Chest. 1989;96(1):68–73.
12. Senn L, Robinson JO, Schmidt S, Knaup M, Asahi N, Satomura S, et al. 1,3-Beta-D-glucan antigenemia for early diagnosis of invasive fungal infections in neutropenic patients with acute leukemia. Clin Infect Dis. 2008;46(6):878–85.
13. Persat F, Ranque S, Derouin F, Michel-Nguyen A, Picot S, Sulahian A. Contribution of the (1–>3)-beta-D-glucan assay for diagnosis of invasive fungal infections. J Clin Microbiol. 2008;46(3):1009–13.
14. Meissner F, Seger RA, Moshous D, Fischer A, Reichenbach J, Zychlinsky A. Inflammasome activation in NADPH oxidase defective mononuclear phagocytes from patients with chronic granulomatous disease. Blood. 2010;116(9):1570–3.
15. Bogaert P, Tournoy KG, Naessens T, Grooten J. Where asthma and hypersensitivity pneumonitis meet and differ: noneosinophilic severe asthma. Am J Pathol. 2009;174(1):3–13.
16. Khaldi H, Marchand-Adam S, Kannengiesser C, Fabre A, Debray MP, Danel C, et al. Diffuse interstitial pneumonia and pulmonary hypertension: a novel manifestation of chronic granulomatous disease. Eur Respir J. 2009;33(6):1498–502.
17. Shah A. Aspergillus-associated hypersensitivity respiratory disorders. Indian J Chest Dis Allied Sci. 2008;50(1):117–28.
18. Van Hoeyveld E, Dupont L, Bossuyt X. Quantification of IgG antibodies to Aspergillus fumigatus and pigeon antigens by ImmunoCAP technology: an alternative to the precipitation technique? Clin Chem. 2006;52(9):1785–93.
19. Lacasse Y, Selman M, Costabel U, Dalphin JC, Morell F, Erkinjuntti-Pekkanen R, et al. Classification of hypersensitivity pneumonitis: a hypothesis. Int Arch Allergy Immunol. 2009;149(2):161–6.
20. Buchvald F, Petersen BL, Damgaard K, Deterding R, Langston C, Fan LL, et al. Frequency, treatment, and functional outcome in children with hypersensitivity pneumonitis. Pediatr Pulmonol. 2011;46(11):1098–107.
21. Dostert C, Petrilli V, Van Bruggen R, Steele C, Mossman BT, Tschopp J. Innate immune activation through Nalp3 inflammasome sensing of asbestos and silica. Science. 2008;320(5876):674–7.
22. Segal BH, Han W, Bushey JJ, Joo M, Bhatti Z, Feminella J, et al. NADPH oxidase limits innate immune responses in the lungs in mice. PLoS One. 2010;5(3):e9631.
23. Takeuchi O, Akira S. Toll-like receptors; their physiological role and signal transduction system. Int Immunopharmacol. 2001;1(4):625–35.
24. Olsson S, Sundler R. The macrophage beta-glucan receptor mediates arachidonate release induced by zymosan: essential role for Src family kinases. Mol Immunol. 2007;44(7):1509–15.
25. Marciano BE, Rosenzweig SD, Kleiner DE, Anderson VL, Darnell DN, Anaya-O'Brien S, et al. Gastrointestinal involvement in chronic granulomatous disease. Pediatrics. 2004;114(2):462–8.
26. Palumbo A, Facon T, Sonneveld P, Blade J, Offidani M, Gay F, et al. Thalidomide for treatment of multiple myeloma: 10 years later. Blood. 2008;111(8):3968–77.
27. Meierhofer C, Wiedermann CJ. New insights into the pharmacological and toxicological effects of thalidomide. Curr Opin Drug Discov Dev. 2003;6(1):92–9.
28. Marks DJ, Miyagi K, Rahman FZ, Novelli M, Bloom SL, Segal AW. Inflammatory bowel disease in CGD reproduces the clinicopathological features of Crohn's disease. Am J Gastroenterol. 2009;104(1):117–24.
29. Keller M, Sollberger G, Beer HD. Thalidomide inhibits activation of caspase-1. J Immunol. 2009;183(9):5593–9.
30. Eski M, Sahin I, Sengezer M, Serdar M, Ifran A. Thalidomide decreases the plasma levels of IL-1 and TNF following burn injury: is it a new drug for modulation of systemic inflammatory response. Burns. 2008;34(1):104–8.
31. Yasui K, Yashiro M, Tsuge M, Manki A, Takemoto K, Yamamoto M, et al. Thalidomide dramatically improves the symptoms of early-onset sarcoidosis/Blau syndrome: its possible action and mechanism. Arthritis Rheum. 2010;62(1):250–7.

Clinical Immunology (2014) 151, 25

available at www.sciencedirect.com

Clinical Immunology

www.elsevier.com/locate/yclim

BRIEF COMMUNICATION

Augmentation of antitubercular therapy with IFNγ in a patient with dominant partial IFNγ receptor 1 deficiency

Kanako Takeda[a], Toshinao Kawai[b,*], Yumiko Nakazawa[b], Hisako Komuro[a], Kensuke Shoji[c], Kumiko Morita[d], Tomohiro Katsuta[e], Matsuri Yamamoto[b], Isao Miyairi[c], Yukihiro Ohya[d], Akira Ishiguro[a], Masafumi Onodera[b]

[a] *Department of General Pediatrics and Interdisciplinary Medicine, National Center for Child Health and Development, Tokyo, Japan*
[b] *Department of Human Genetics, National Center for Child Health and Development, Tokyo, Japan*
[c] *Division of Infectious Diseases, Department of Medical Subspecialties, National Center for Child Health and Development, Tokyo, Japan*
[d] *Division of Allergy, Department of Medical Subspecialties, National Center for Child Health and Development, Tokyo, Japan*
[e] *Department of Pediatrics, St. Marianna University School of Medicine, Kanagawa, Japan*

Received 1 October 2013; accepted with revision 4 January 2014

KEYWORDS
Mendelian susceptibility to mycobacterial diseases;
Interferon-γ receptor 1 deficiency;
Mycobacterium bovis Bacille Calmette–Guerin;
Osteomyelitis;
Interferon-γ

Abstract Osteomyelitis due to *Mycobacterium bovis* Bacille Calmette–Guerin (BCG) often develops in patients with interferon-γ receptor 1 (IFNγR1) deficiency. In these patients, susceptibility appears to be caused by impaired interleukin-12- and IFNγ-mediated immunity. Here we report the case of a one-year-old girl with dominant partial IFNγR1 deficiency who suffered from lymphadenitis and multiple sites of osteomyelitis due to BCG infection. She was allergic to isoniazid and rifampicin – the prescribed standard treatment – and required prior desensitization therapy. She was subsequently treated with these drugs, but her symptoms did not improve. IFNγ therapy was added to the antitubercular therapy, increasing the serum level of IFNγ and leading to the resolution of the lymphadenitis and osteomyelitis. In conclusion, high dose IFNγ therapy in combination with antitubercular drugs led to resolution of BCG infection in a patient with dominant partial IFNγ deficiency.

1. Introduction

Mendelian susceptibility to mycobacterial disease (MSMD) is a rare primary immunodeficiency characterized by a deficiency in the interleukin (IL)-12/23–interferon-γ (IFNγ)

* Corresponding author at: Department of Human Genetics, National Center for Child Health and Development, 2-10-1 Okura, Setagaya-ku, Tokyo 157-8535, Japan. Fax: +81 3 5494 7035.
E-mail address: kawai-t@ncchd.go.jp (T. Kawai).

1521-6616/$ - see front matter © 2014 Elsevier Inc. All rights reserved.
http://dx.doi.org/10.1016/j.clim.2014.01.004

axis. Type-1 cytokine response is crucial for human host defense against intracellular pathogens. Patients with MSMD demonstrate increased susceptibility to infections of environmental non-tuberculous mycobacteria, *Salmonella* and *Mycobacterium bovis* (*M. bovis*) Bacille Calmette–Guerin (BCG) [1,2]. Several genetic mutations have been identified in patients with MSMD. Mutations have been found in genes coding for IL-12β, IL-12 receptor β1, IFNγ receptor 1 (IFNγR1), IFNγ receptor 2 (IFNγR2), signal transducers and activator of transcription (STAT1), NF-κB essential modulator (NEMO), gp91phox, tyrosine kinase 2 (TYK2), interferon regulatory factor 8 (IRF8) and interferon-stimulated gene 15 protein (ISG15). The 818del4 mutation of *IFNGR1* gene results in a truncated protein that exerts a dominant negative effect on the wild-type IFNγR1 molecule. Accumulation of truncated IFNγR1 proteins impedes the function of normal IFNγR1 molecules encoded by the wild-type allele [3,4], leading to a diminished cellular response to ligand binding. Previous reports have shown that BCG causes recurrent and refractory osteomyelitis in patients with dominant partial IFNγR1 deficiency [5–8]. Among vaccinated children, almost 70% of those with dominant partial IFNγR1 deficiency develop osteomyelitis due to BCG [1].

Standard therapy caused by *M. bovis*, recommended by the Centers for Disease Control and Prevention (CDC) and the American Academy of Pediatrics (AAP), is a multidrug regimen that includes isoniazid, rifampin and ethambutol (*M. bovis* is inherently resistant to pyrazinamide). However, in patients with dominant partial IFNγR1 deficiency develop osteomyelitis, BCG infection is relatively resistant to this type of therapy [1,6]. Moreover, allergy against such drugs is also present in some cases. Therefore, an alternative approach is necessary for such patients.

Here, we describe a Japanese girl with dominant partial IFNγR1 deficiency who suffered from BCG multiple sites of osteomyelitis and lymphadenitis. She was allergic to isoniazid and rifampicin but was treated with the drugs following desensitization therapy. Unfortunately, standard therapy did not resolve the infection. In light of her genetic background, IFNγ was added to her antitubercular drug regimen. The combination of isoniazid, rifampicin, ethambutol and high dose IFNγ successfully cured her multi-site osteomyelitis and lymphadenitis.

2. Patient and method

The patient, a one-year-old girl (vaccinated with BCG at 2 months of age), suffered from axillary lymphadenitis at 10 months of age. Three months later, she was presented with osteomyelitis at multiple sites, including the skull, humerus, tibia and cervical vertebra (Fig. 1a). Axillary lymph node and skull tissue biopsies revealed the presence of *M. bovis* BCG (BCG Tokyo 172 strain). Immunological assessment was performed to evaluate the presence of primary phagocytic disorders, such as chronic granulomatous disease [9] or MSMD. Flow cytometry revealed a five-fold increase in the expression of IFNγR1 on $CD14^+$ monocytes isolated from the patient (Fig. 1c) (mean fluorescence intensity of IFNγR1: 10371, 51350, and 50583 for a healthy subject, the patient, and the patient's mother, respectively). The diagnosis of dominant partial IFNγR1 deficiency was confirmed by a genetic analysis that revealed one four-nucleotide deletion in exon 6 of *IFNGR1* (818del4) and one wild-type *IFNGR1* allele (Fig. 1d). Interestingly, the patient's mother carried the same *IFNGR1* deletion and suffered from one episode of osteomyelitis and multiple subcutaneous abscesses due to *Mycobacterium* spp. at one year of age, though she did not receive BCG vaccination. The patient and her mother were thus diagnosed with inherited dominant partial IFNγR1 deficiency.

3. Results

3.1. Addition of high dose IFNγ to antitubercular regimen

The patient was initially treated with isoniazid and rifampicin, based on the guidelines of the CDC and AAP. However, she developed generalized erythema multiform exudativum two weeks after commencement of treatment. Consequently, her antitubercular drug regimen was changed to ethambutol and levofloxacin due to the antimicrobial sensitivity to *M. bovis* isolated from her osteomyelitis lesion. This regimen proved ineffective in treating her lymphadenitis and osteomyelitis. We decided to put her on a two-month course of desensitization to isoniazid and rifampicin according to the Guidelines of Japanese Society of Tuberculosis [10]. Desensitization of each drug started at 0.2 mg/kg/day and the dose was doubled every 7–10 days to reach 10 mg/kg/day (Fig. 1e). Although desensitization therapy was successful, the patient failed to improve with this medical regimen.

Upon obtaining informed consent from the family, IFNγ was added to the regimen. IFNγ was initially administered subcutaneously at 250 000 JRU/m^2 per week, a sufficient dose for infection prophylaxis in chronic granulomatous disease [11], and up-titrated thereafter. Treatment with IFNγ resulted in an increase in serum IFNγ level, and a decrease in serum IL-6 level (Fig. 1e) with no change in serum TNFα and IL-12 levels (although the patient's serum TNFα level was higher than that of healthy subjects at baseline: 16.5 ± 4.0 pg/ml vs. 1.1 ± 0.9 pg/ml, respectively, $p < 0.001$). A final dose of 1250 000 JRU/m^2 IFNγ per week led to resolution of her axillary lymphadenitis and ossification of the multiple osteomyelitic lesions (Fig. 1b).

3.2. Assessment of the effect of high dose IFNγ on the patient's immune function

Peripheral blood mononuclear cells (PBMCs) were isolated from the patient, the patient's mother and healthy subjects (n = 3), and stimulated with lipopolysaccharide (LPS) with or without IFNγ. The amount of TNFα produced by the stimulated PBMCs was measured by quantitative multiplex detection using Milliplex (Millipore, Billerica, MA). When PBMCs were stimulated with LPS alone, similar amounts of TNFα were produced (Fig. 2). In PBMCs isolated from healthy donors, the addition of IFNγ led to an increase in TNFα production in a dose-dependent manner; whereas in PBMCs isolated from the patient and her mother, TNFα production increased only when IFNγ was added at the maximum concentration (10^5 JRU/mL) (Fig. 2).

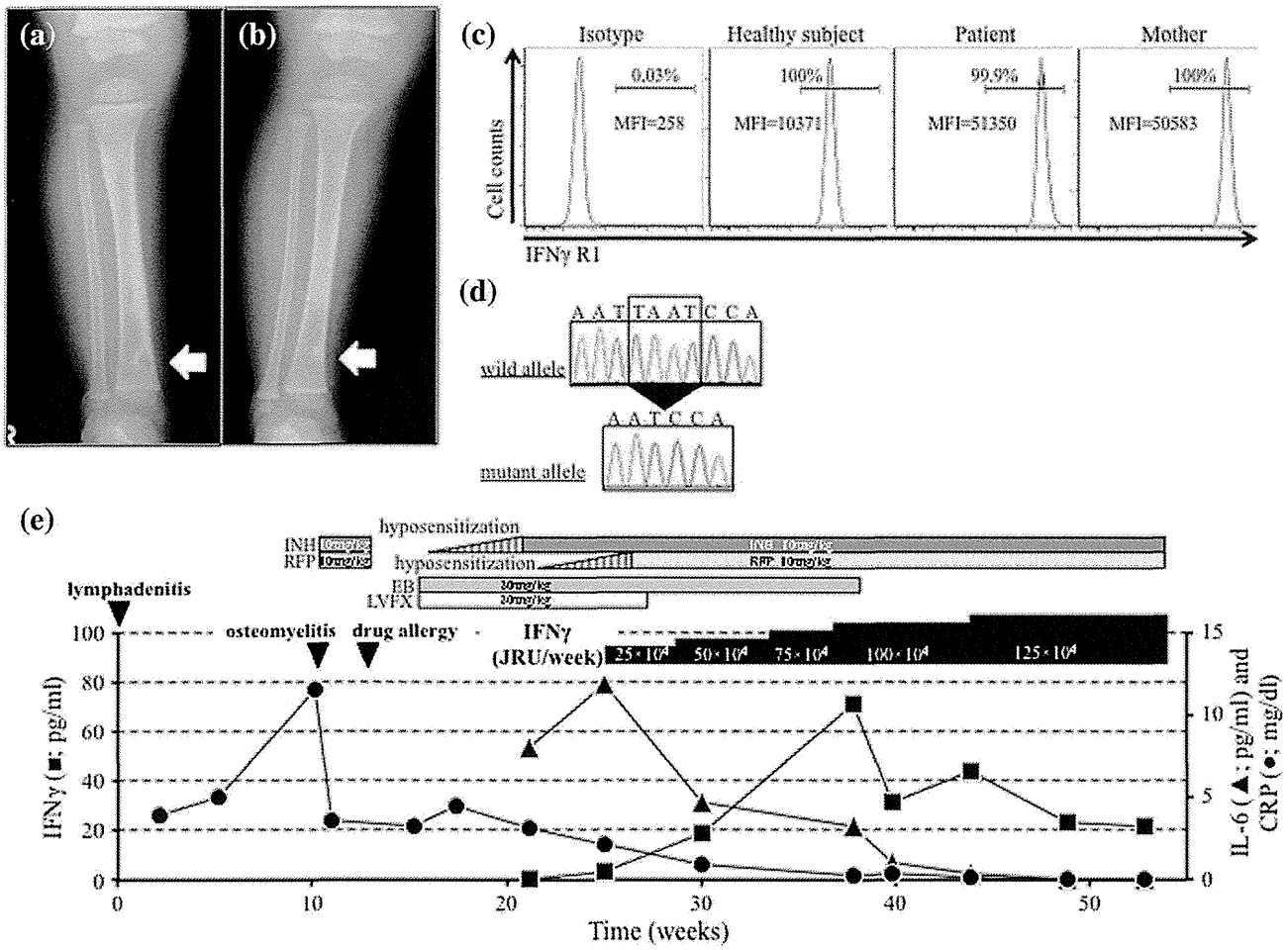

Figure. 1 Clinical course of BCG osteomyelitis in a patient with dominant partial IFNγ receptor 1 deficiency. (a)–(b) X-rays demonstrating osteomyelitis of the right tibia before IFNγ administration (a) and ossification of the lesion following IFNγ therapy (b). (c) Representative flow cytometry data. PBMCs were identified with FACSAria IIIu using anti-human CD14 and IFNγR1 monoclonal antibodies conjugated with allophycocyanin and phycoerythrin, respectively (BioLegend, San Diego, CA). MFI, mean fluorescence intensity. (d) Genetic analysis of the patient's genomic DNA revealed a 4-nucleotide deletion in exon 6 of *IFNGR1* (818del4) and a wild-type *IFNGR1* allele. (e) Clinical time course of treatment with IFNγ and multidrug antitubercular therapy. Serum levels of IFNγ (squares), IL-6 (triangles), and CRP (circles) were assessed during treatment.

4. Discussion

In the patients with dominant partial IFNγR1 deficiency, BCG infection is relatively resistant to conventional antitubercular therapy, although the clinical features of dominant partial IFNγR1 deficiency are less severe than those of complete deficiency [1,6]. Our data indicated that a high dose of IFNγ was capable of restoring the patient's impaired immune response to BCG infection. Superphysiologic IFNγ can overcome the dominant negative effect of truncated IFNγ by binding to the dimerized residual wild-type receptor, leading to the production of STAT1 associated-cytokines such as IFNγ, TNFα, IL-12 and IL-6 [7,12]. We found that in PBMCs from the patient and her mother, high dose IFNγ enhanced LPS-induced TNFα production.

Interestingly, PBMCs from the patient and her mother produced as much TNFα as healthy PBMCs in response to LPS alone. This suggests that the TLR4 signaling axis remains intact in PBMCs from patients with dominant partial IFNγR1 deficiency. It should be noted that serum TNFα levels were elevated in the patient but not in her mother, indicating residual BCG infection even in the context of normal serum IL-6 and C-reactive protein (CRP) levels. Collectively, these findings show that TNFα levels may be a useful measure of infection severity in patients with dominant partial IFNγR1 deficiency.

5. Conclusion

We have demonstrated that high dose IFNγ, when added to standard antitubercular regimen, is effective in the treatment of multi-site osteomyelitis and lymphadenitis in patients with dominant partial IFNγ deficiency.

Conflict of interest

The authors declare that they have no conflicts of interest.

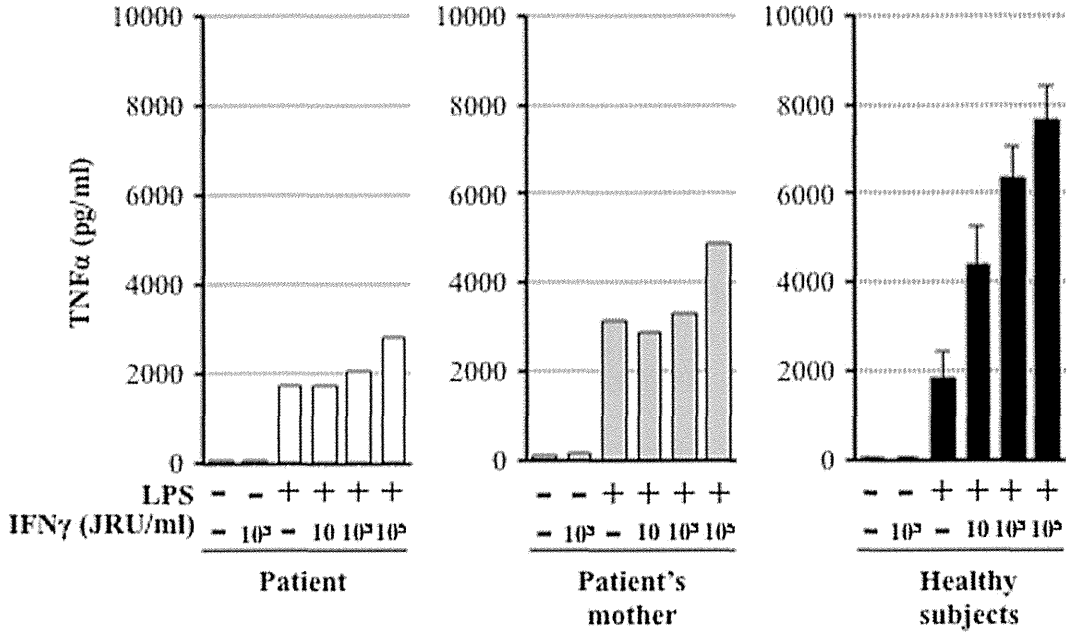

Figure. 2 TNFα production in response to LPS plus IFNγ in PBMCs. PBMCs isolated from the patient (white bars), patient's mother (gray bars), and healthy subjects (black bars) were stimulated with LPS alone or LPS plus serial concentration of IFNγ for 20 h. The level of TNFα in culture supernatant was measured by quantitative multiplex detection using Milliplex.

Acknowledgments

We are grateful to the patients with IFNγR1 deficiency who participated in this study. The manuscript was proofread and edited by Dr. Julian Tang of the Department of Clinical Research Education, National Center for Child Health and Development. The work was supported by grants from the Ministry of Health, Labor and Welfare and the National Center for Child Health and Development.

References

[1] S.E. Dorman, C. Picard, D. Lammas, K. Heyne, J.T. van Dissel, R. Baretto, S.D. Rosenzweig, M. Newport, M. Levin, J. Roesler, D. Kumararatne, J.L. Casanova, S.M. Holland, Clinical features of dominant and recessive interferon gamma receptor 1 deficiencies, Lancet 364 (2004) 2113–2121.

[2] M.H. Haverkamp, E. van de Vosse, J.T. van Dissel, Nontuberculous mycobacterial infections in children with inborn errors of the immune system, J. Infect. 68 (2014) S134–S150.

[3] E. Jouanguy, S. Lamhamedi-Cherradi, D. Lammas, S.E. Dorman, M.C. Fondaneche, S. Dupuis, R. Doffinger, F. Altare, J. Girdlestone, J.F. Emile, H. Ducoulombier, D. Edgar, J. Clarke, V.A. Oxelius, M. Brai, V. Novelli, K. Heyne, A. Fischer, S.M. Holland, D.S. Kumararatne, R.D. Schreiber, J.L. Casanova, A human IFNGR1 small deletion hotspot associated with dominant susceptibility to mycobacterial infection, Nat. Genet. 21 (1999) 370–378.

[4] S.M. Arend, R. Janssen, J.J. Gosen, H. Waanders, T. de Boer, T.H. Ottenhoff, J.T. van Dissel, Multifocal osteomyelitis caused by nontuberculous mycobacteria in patients with a genetic defect of the interferon-gamma receptor, Neth. J. Med. 59 (2001) 140–151.

[5] K. Obinata, T. Lee, T. Niizuma, K. Kinoshita, T. Shimizu, T. Hoshina, Y. Sasaki, T. Hara, Two cases of partial dominant interferon-gamma receptor 1 deficiency that presented with different clinical courses of bacille Calmette–Guerin multiple osteomyelitis, J. Infect. Chemother. 19 (2013) 757–760.

[6] T. Hoshina, H. Takada, Y. Sasaki-Mihara, K. Kusuhara, K. Ohshima, S. Okada, M. Kobayashi, O. Ohara, T. Hara, Clinical and host genetic characteristics of Mendelian susceptibility to mycobacterial diseases in Japan, J. Clin. Immunol. 31 (2011) 309–314.

[7] E. Jouanguy, F. Altare, S. Lamhamedi, P. Revy, J.F. Emile, M. Newport, M. Levin, S. Blanche, E. Seboun, A. Fischer, J.L. Casanova, Interferon-gamma-receptor deficiency in an infant with fatal bacille Calmette–Guerin infection, N. Engl. J. Med. 335 (1996) 1956–1961.

[8] J.L. Casanova, E. Jouanguy, S. Lamhamedi, S. Blanche, A. Fischer, Immunological conditions of children with BCG disseminated infection, Lancet 346 (1995) 581.

[9] T. Kawai, H. Kusakabe, A. Seki, S. Kobayashi, M. Onodera, Osteomyelitis due to trimethoprim/sulfamethoxazole-resistant *Edwardsiella tarda* infection in a patient with X-linked chronic granulomatous disease, Infection 39 (2011) 171–173.

[10] Y. Kobashi, T. Abe, E. Shigeto, S. Yano, T. Kuraoka, M. Oka, Desensitization therapy for allergic reactions to antituberculous drugs, Intern. Med. 49 (2010) 2297–2301.

[11] B. Martire, R. Rondelli, A. Soresina, C. Pignata, T. Broccoletti, A. Finocchi, P. Rossi, M. Gattorno, M. Rabusin, C. Azzari, R.M. Dellepiane, M.C. Pietrogrande, A. Trizzino, P. Di Bartolomeo, S. Martino, L. Carpino, F. Cossu, F. Locatelli, R. Maccario, P. Pierani, M.C. Putti, A. Stabile, L.D. Notarangelo, A.G. Ugazio, A. Plebani, D. De Mattia, Ipinet, Clinical features, long-term follow-up and outcome of a large cohort of patients with chronic granulomatous disease: an Italian multicenter study, Clin. Immunol. 126 (2008) 155–164.

[12] M.J. Newport, C.M. Huxley, S. Huston, C.M. Hawrylowicz, B.A. Oostra, R. Williamson, M. Levin, A mutation in the interferon-gamma-receptor gene and susceptibility to mycobacterial infection, N. Engl. J. Med. 335 (1996) 1941–1949.

Cancer Science
Japanese Cancer Association JCA
Open Access

Anti-tumor effects of suberoylanilide hydroxamic acid on Epstein–Barr virus-associated T cell and natural killer cell lymphoma

Mohammed N.A. Siddiquey,[1] Hikaru Nakagawa,[1] Seiko Iwata,[1] Tetsuhiro Kanazawa,[1] Michio Suzuki,[1,2] Ken-Ichi Imadome,[3] Shigeyoshi Fujiwara,[3] Fumi Goshima,[1] Takayuki Murata[1] and Hiroshi Kimura[1]

Departments of [1]Virology, [2]Pediatrics, Nagoya University Graduate School of Medicine, Nagoya; [3]Department of Infectious Diseases, National Research Institute for Child Health and Development, Tokyo, Japan

Key words

Extranodal NK-T-cell lymphoma, histone deacetylase inhibitor, human herpesvirus 4, hydroxamic acid, SCID mice

Correspondence

Hiroshi Kimura, Department of Virology, Nagoya University Graduate School of Medicine, 65 Tsurumai-cho, Showa-ku, Nagoya 466-8550, Japan.
Tel: +81-52-744-2207; Fax: +81-52-744-2452;
E-mail: hkimura@med.nagoya-u.ac.jp

Funding information

Ministry of Education, Culture, Sports, Science and Technology of Japan (25293109). Ministry of Health, Labour and Welfare of Japan (H24-Nanchi-046).

Received February 26, 2014; Revised March 31, 2014; Accepted April 7, 2014

Cancer Sci **105** (2014) 713–722

doi: 10.1111/cas.12418

The ubiquitous Epstein–Barr virus (EBV) infects not only B cells but also T cells and natural killer (NK) cells and is associated with various lymphoid malignancies. Recent studies have reported that histone deacetylase (HDAC) inhibitors exert anticancer effects against various tumor cells. In the present study, we have evaluated both the *in vitro* and *in vivo* effects of suberoylanilide hydroxamic acid (SAHA), an HDAC inhibitor, on EBV-positive and EBV-negative T and NK lymphoma cells. Several EBV-positive and EBV-negative T and NK cell lines were treated with various concentrations of SAHA. SAHA suppressed the proliferation of T and NK cell lines, although no significant difference was observed between EBV-positive and EBV-negative cell lines. SAHA induced apoptosis and/or cell cycle arrest in several T and NK cell lines. In addition, SAHA increased the expression of EBV-lytic genes and decreased the expression of EBV-latent genes. Next, EBV-positive NK cell lymphoma cells were subcutaneously inoculated into severely immunodeficient NOD/Shi-scid/IL-2Rγnull mice, and then SAHA was administered intraperitoneally. SAHA inhibited tumor progression and metastasis in the murine xenograft model. SAHA displayed a marked suppressive effect against EBV-associated T and NK cell lymphomas through either induction of apoptosis or cell cycle arrest, and may represent an alternative treatment option.

More than 90% of the world population is infected by the Epstein–Barr virus (EBV), which is an oncogenic γ-herpesvirus. Not only B cells but also T cells and natural killer (NK) cells can be infected by EBV, a condition that is associated with various lymphoid malignancies, including Burkitt lymphoma, Hodgkin lymphoma, post-transplant lymphoproliferative disorders, extranodal NK/T cell lymphoma, hydroa vacciniforme-like lymphoma, aggressive NK cell leukemia and chronic active EBV infection.[1,2] The ability of EBV to establish latent infection and induction of the proliferation of infected cells make it the significant causative agent in the pathogenesis of many of these malignancies. Some of these EBV-associated T and NK cell malignancies are refractory to conventional chemotherapies and have poor prognoses.[3] For the treatment and prophylaxis of B cell lymphoma and lymphoproliferative disorders, rituximab, a humanized monoclonal antibody (Ab) against CD20, targets B cell-specific surface antigens and has been used with marked success.[4,5] However, novel approaches to molecular targeted therapy are required to effectively treat T and NK cell malignancies.

Histone deacetylase (HDAC) inhibitors induce acetylation of histones, thus affecting transcription, and selectively induce tumor-suppressive genes. In various cancer cell types, HDAC inhibitors induce differentiation, apoptosis and cell cycle arrest.[6,7] Moreover, with notable tumor specificity, HDAC inhibitors have potent anticancer activities, and some exhibit therapeutic potential through their targeting of epigenetic regulation. Previously, we showed that an HDAC inhibitor, valproic acid, induced apoptosis and cell cycle arrest in EBV-positive T and NK lymphoma cells.[8] However, the suppressive effect of valproic acid in cell lines was modest and was not affected by the presence of EBV.

Suberoylanilide hydroxamic acid (SAHA) is an FDA-approved HDAC inhibitor, and its efficacy has been confirmed by clinical trials for malignant diseases such as non-Hodgkin lymphoma, acute myeloid leukemia, breast cancer and cutaneous T cell lymphoma.[9–12] Micromolar concentrations of SAHA have anticancer effects and a well-established safety profile.[9] Furthermore, recent studies have confirmed that SAHA can induce EBV lytic infection and mediate enhanced cell death in EBV-positive gastric carcinoma and nasopharyngeal carcinoma cells.[13,14] Very recently, a gene expression profile study identified SAHA as an effective drug candidate for NK cell neoplasms, including EBV-positive NK lymphoma.[15] However, no *in vivo* study has evaluated the efficacy of SAHA in EBV-positive T and NK lymphoma cells.

In the present study, we evaluate the antitumor effects of SAHA on EBV-positive and EBV-negative T and NK cell lines

and analyze induction of apoptosis, cell cycle arrest and expression of EBV-encoded genes. To further evaluate the effect of SAHA, an *in vivo* model is necessary. A suitable host for xenotransplantation of human lymphoid cells is the NOD/Shi-*scid*/IL-2Rγ^{null} (NOG) mouse, which is completely immunodeficient and lacks T, B, NK and dendritic cells, as well as macrophages.[16–19] Recently, the proliferation of EBV-positive T and NK cells has been confirmed by the xenotransplantation of human peripheral blood mononuclear cells (PBMC) to the NOG mouse.[20] Instead of human PBMC, we applied the xenograft model to evaluate SAHA using an EBV-positive NK cell line, which is more suitable for the evaluation of drugs.

Materials and Methods

Cell lines. Of the cell lines used, SNT13 and SNT16 are EBV-positive T cell lines,[21] Jurkat is an EBV-negative T cell line,[22] KAI3 and SNK6 are EBV-positive NK cell lines,[21,23] and KHYG1 is an EBV-negative NK cell line.[24] EBV-positive MT2/rEBV/9-7 and MT2/rEBV/9-9 cell lines were established by infection of MT2 cells with the hygromycin-resistant B95-8 strain.[25,26] EBV-negative MT2/hyg/CL2 and MT2/hyg/CL3 cell lines were transfected with a hygromycin-resistant gene. These four cell lines were used to verify the presence/absence of EBV in the T cell lines. Similarly, the EBV-negative NKL cell line was derived from a patient with NK cell leukemia, and the EBV-positive TL1 cell line was established from NKL cells infected with an Akata-transfected recombinant EBV strain containing a neomycin-resistant gene.[27,28] TL1 and NKL were used to verify the presence/absence of EBV in the NK cell lines. The characteristics of each cell line are summarized in Table 1.

Jurkat cells were cultured in RPMI 1640 medium supplemented with 10% FBS, penicillin, streptomycin and glutamine (complete medium). SNT13, SNT16, KAI3, SNK6, KHYG1, TL1 and NKL cells were grown in complete medium supplemented with 100 U/mL human interleukin-2 (IL-2). MT2/rEBV/9-7, MT2/rEBV/9-9, MT2/hyg/CL2 and MT2/hyg/CL3 cells were grown in complete medium supplemented with 0.2 mg/mL hygromycin. For xenotransplantation, the SNK6 cell line was grown in complete medium supplemented with human serum and 700 U/mL of human IL-2. All cultures were maintained at 37°C in 5% CO_2.

Cell viability. Suberoylanilide hydroxamic acid (Cayman Chemicals, Ann Arbor, MI, USA) was dissolved in DMSO. Each cell line (2×10^5 cells per mL) was cultured in 24-well plates. Human PBMC were isolated from healthy volunteers using Ficoll–Paque (GE Heathcare AB BioSciences, Uppsala, Sweden) gradient centrifugation, and 5×10^5 PBMC per mL were cultured in 24-well plates. Cells were treated with various concentrations of SAHA for 96 h. The cell number and viability were quantified by trypan blue exclusion. Viability was calculated as the percentage of viable SAHA-treated cells versus DMSO-treated cells. These experiments were performed in triplicate, and the results were expressed as mean values with SEM.

Table 1. Characteristics of the cell lines

Name	Cell type	EBV	Cell origin
SNT13	T	+	Chronic active EBV infection
SNT16	T	+	Chronic active EBV infection
Jurkat	T	–	Acute T lymphoblastic leukemia
KAI3	NK	+	Chronic active EBV infection
SNK6	NK	+	Extranodal NK/T cell lymphoma
KHYG1	NK	–	Aggressive NK cell leukemia
MT2/rEBV/9-7	T	+	MT2 cell line
MT2/rEBV/9-9	T	+	MT2 cell line
MT2/hyg/CL2	T	–	MT2 cell line
MT2/hyg/CL3	T	–	MT2 cell line
TL1	NK	+	NKL cell line
NKL	NK	–	NK-cell leukemia

EBV, Epstein–Barr virus; NK, natural killer.

Apoptosis assay by flow cytometry. Apoptosis was measured by flow cytometry using an annexin V-PE/7-AAD apoptosis assay kit (BD Pharmingen Biosciences, San Diego, CA, USA) according to the manufacturer's protocol.[29] Briefly, 2×10^5 cells were treated with SAHA for 24 h, incubated with annexin V-PE and 7-AAD for 15 min, and then analyzed by flow cytometry. Stained cells were analyzed using the FACSCantoII flow cytometer and the FlowJo software (Tree Star, Ashland, OR, USA).

Immunoblotting. After 24 and 48 h of treatment with various concentrations of SAHA, cell pellets were lysed directly in SDS sample buffer (50 mM Tris-HCl [pH 6.8], 2% SDS, 10% glycerol, 6% 2-mercaptoethanol and 0.0025% bromophenol blue). Cell lysates were separated on 10% acrylamide gels by SDS-PAGE, transferred to PVDF membranes, and immunoblotted with Abs. Abs were used against acetyl-histone H3 (Cell Signaling, Boston, MA, USA), poly (ADP-ribose) polymerase (PARP; Sigma, St. Louis, MO, USA), latent membrane protein (LMP) 1 (S12; BD Biosciences, San Jose, CA, USA),[30] EBV nuclear antigen (EBNA) 1[31] and β-actin (Sigma).

Cell cycle assay. Cells were treated with various concentrations of SAHA for 48 h and fixed with 70% ethanol. Fixed cells were treated with DNase-free RNase, stained with propidium iodide (Sigma) for 15 min, and analyzed by flow cytometry. Stained cells were analyzed using a FACSCalibur (Becton Dickinson, San Jose, CA, USA) flow cytometer and the ModFit LT software (Verity Software House, Topsham, ME, USA).

RT-PCR assay. RNA was extracted using the QIAmp RNeasy Mini Kit (Qiagen, Hilden, Germany), and contaminating DNA was removed by on-column DNase digestion using the RNase-free DNase Set (Qiagen). Viral mRNA expression was quantified by one-step multiplex real-time RT-PCR using the Mx3000P real-time PCR system (Stratagene, La Jolla, CA, USA) as described previously.[32,33] β2-Microglobulin was used as an endogenous control and reference gene for relative quantification.[34] Each experiment was performed in triplicate and was shown as the mean of three samples with the SEM.

Xenograft model using the NOG mouse. Female 6-week-old or 7-week-old NOG mice were obtained from the Central Institute of Experimental Animals, Kawasaki, Japan, and maintained under specific pathogen-free conditions by the approval and guidelines of the Nagoya University Experimentation Animal Committee. On day 0, 1×10^6 SNK6 cells were inoculated subcutaneously as described previously.[35] Each day from days 4 to 28, the mice were treated i.p. with 100 mg/kg SAHA or DMSO (control). Tumor volume was quantified using calipers twice per week and calculated using the following formula: $\pi \times$ short axis $\times$ long axis $\times$ height/6. On day 30, mice were killed, and the tumor and organs were excised. RNA was extracted from the tumor and subjected to real-time RT-PCR to quantify viral gene expression. Peripheral blood was collected, and plasma was separated. DNA was extracted from the plasma and quantified by quantitative real-time PCR.[36]

The Mann–Whitney *U*-test was used to compare tumor volumes, viral mRNA expression and quantity of EBV-DNA. *P*-values <0.05 were deemed to indicate statistical significance.

Epstein–Barr virus-encoded small RNA *in situ* hybridization. Formalin (20%)-fixed and sucrose (0.1%)-fixed tissues were sectioned into 10-μm slices and treated with 1:10 diluted proteinase K. The tissues were incubated at room temperature for 30 min, and were then washed with pure water and ethanol (96%). The tissues were stained for Epstein–Barr virus-encoded small RNA (EBER) by *in situ* hybridization (ISH). EBER-ISH was performed using the EBER PNA Probe (Y5200; Dako) and the PNA ISH detection kit (Dako, Glostrup Denmark) according to the manufacturer's protocol.[33]

Results

Effect of suberoylanilide hydroxamic acid on the viability of T and natural killer cell lines. Epstein–Barr virus-positive and EBV-negative T and NK cell lines were cultured with various concentrations of SAHA. SAHA increased acetylated histone H3 levels, confirming that SAHA worked as an HDAC inhibitor (Fig. 1a). SAHA reduced the viability of all treated cell lines in a dose-dependent manner (Fig. 1b). Next, the same six cell lines were treated with 5 μM SAHA and assessed at different time points. The viability of all six cell lines was reduced by treatment with SAHA for 96 h (Fig. 1c). The effects of SAHA did not differ between EBV-positive and EBV-negative cell lines. In addition, to compare its effects on EBV-positive and EBV-negative cell lines, we treated MT2/rEBV/9-7 and MT2/rEBV/9-9 cells (EBV-positive T cell lines), MT2/hyg/CL2 and MT2/hyg/CL3 cells (EBV-negative T cell lines), TL1 cells (EBV-positive NK cell line) and NKL cells (EBV-negative parental NK cell line) with SAHA. SAHA had similar effects on the EBV-positive and EBV-negative cell lines (Fig. 2a). Moreover, human PBMC were treated with SAHA to evaluate the adverse effects. Viability remained >69% at 96 h, indicating the absence of adverse effects (Fig. 2b).

Effects of suberoylanilide hydroxamic acid on apoptosis and the cell cycle of T and natural killer cell lines. To determine whether apoptosis was induced by SAHA in the tested cell lines, early apoptotic cells were quantified by annexin V and 7-AAD staining. SAHA increased early apoptotic cells in the Jurkat, KAI3 and KHYG1 cell lines (Fig. 3a). In other cell lines, the proportions of early apoptotic cells were not increased. Next, the cleavage of PARP was analyzed by immunoblotting. With the exception of the SNT16 cell line, SAHA induced the cleavage of PARP in the five cell lines (Fig. 3b). Next, effects on the cell cycle were investigated. In the SNT16 and KAI3 cell lines, the population of cells in G1 phase was increased, whereas that in G2 phase was increased in the SNK6 cell line (Fig. 4). In Jurkat and KHYG1 cells, the cell cycle assay was indeterminate because of the massive cell death caused by SAHA.

Effects of suberoylanilide hydroxamic acid on Epstein–Barr virus-encoded genes of Epstein–Barr virus-positive T and natural killer cell lines. The expression of eight EBV-related genes, including lytic genes (BZLF1 and gp350/220) and latent genes (EBNA1, EBNA2, LMP1, LMP2, EBER1 and Bam HI-A rightward transcripts [BART]) were analyzed using real-time RT-PCR. In the SNT13, KAI3 and SNK6 cell lines, the

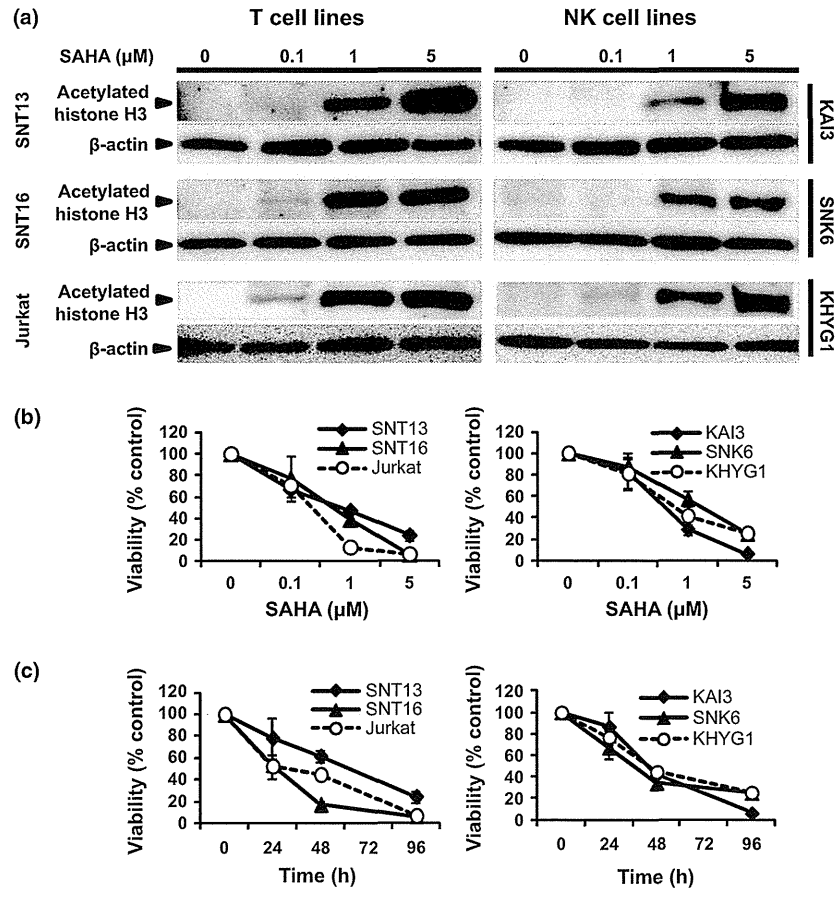

Fig. 1. Suberoylanilide hydroxamic acid (SAHA) inhibits the deacetylation of histone H3 protein and decreases the viability of T and natural killer (NK) cell lines. (a) SNT13, SNT16 (Epstein–Barr virus [EBV]-positive T cell line), Jurkat (EBV-negative T cell line), KAI3, SNK6 (EBV-positive NK cell line) and KHYG1 (EBV-negative NK cell line) cells were treated with the indicated SAHA concentrations for 24 h, and acetylated histone H3 was detected by immunoblotting. β-Actin was used as a loading control. (b) Each cell line was treated with the indicated concentrations of SAHA for 96 h or (c) with 5 μM SAHA for the indicated times. Data are expressed as means ± SEM.

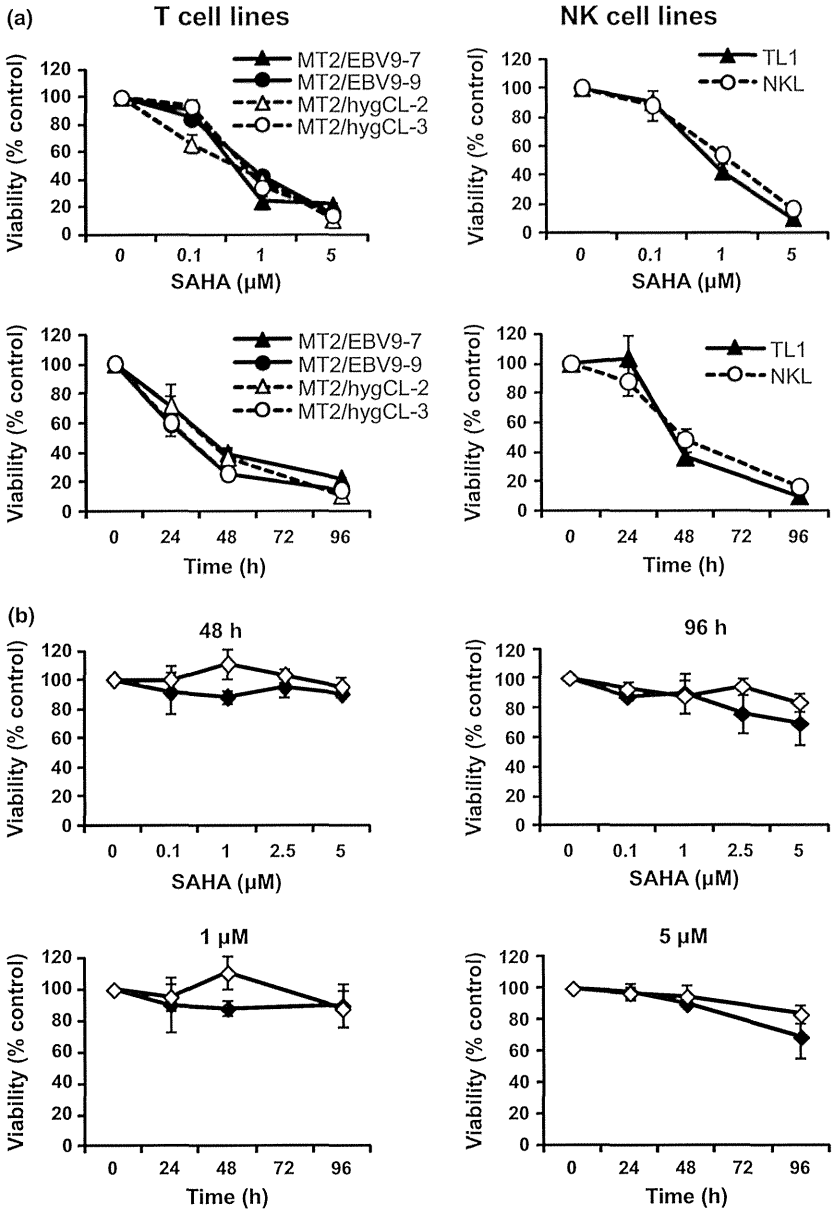

Fig. 2. The effects of suberoylanilide hydroxamic acid (SAHA) do not differ between Epstein–Barr virus (EBV)-positive and EBV-negative cell lines, and SAHA exerts no adverse effects on human peripheral blood mononuclear cells (PBMC). (a) MT2/rEBV/9-7, MT2/rEBV/9-9 (EBV-positive T cell lines), MT2/hyg/CL2, MT2/hyg/CL3 (parental cell lines), TL1 (EBV-positive natural killer [NK] cell line) and NKL (parental cell line) cells were treated with the indicated concentrations of SAHA for 96 h or with 5 μM SAHA for the indicated times. (b) Human PBMC were isolated from two volunteers and treated with the indicated concentrations of SAHA for 48 and 96 h or with 1 and 5 μM SAHA for the indicated times. Data are expressed as means ± SEM.

expression of BZLF1, which is an immediate-early gene in the lytic infection cycle, was increased by SAHA (Fig. 5). However, the expression of the late lytic gene gp350/220 was increased only in the SAHA-treated SNT13 cell line. These results indicated that SAHA induced lytic infection in some EBV-positive T and NK cell lines, although it was abortive. The expression of BZLF1 was decreased in the SAHA-treated SNT16 as time went by, while that in mock-treated SNT16 was also decreased. Of the EBV latent genes tested, the expression of EBNA1, LMP1 and BART was decreased in most of the cell lines, whereas that of LMP2 was increased by SAHA (Fig. 5). Next, the EBNA1 and LMP1 protein levels were determined by immunoblotting. SAHA decreased the EBNA1 protein level in all cell lines, and that of LMP1 in the SNT16, KAI3 and SNK6 cell lines (Fig. 6).

***In vivo* effects of suberoylanilide hydroxamic acid using the mouse xenograft model.** After confirmation of the *in vitro* effect of SAHA, we extended our work to an *in vivo* xenograft model. Initially, we inoculated six T and NK cell lines into immunodeficient NOG mice via various routes. Of the EBV-positive T or NK cell lines used, only the SNK6 cell line was engrafted after subcutaneous or intravenous inoculation (Suppl. Table S1). The Jurkat cell line, which is EBV-negative and IL-2 independent, could also be engrafted, raising the possibility that IL-2 dependency may be associated with the engraftment. We cultured six cell lines with the different concentration of IL-2, and found that SNK6 was less dependent of IL-2 compared with other T/NK cell lines (Suppl. Fig. S1). We considered that the independency of IL-2 can explain the success of engraftment, at least partially. Because evaluation of the former was easier, the subcutaneous model was used in subsequent experiments.

We subcutaneously inoculated 1×10^6 SNK6 cells into NOG mice. All of the mice developed tumors at the site of inoculation. Four days after the inoculation, mice were treated with SAHA daily up to day 28. The treated mice normally

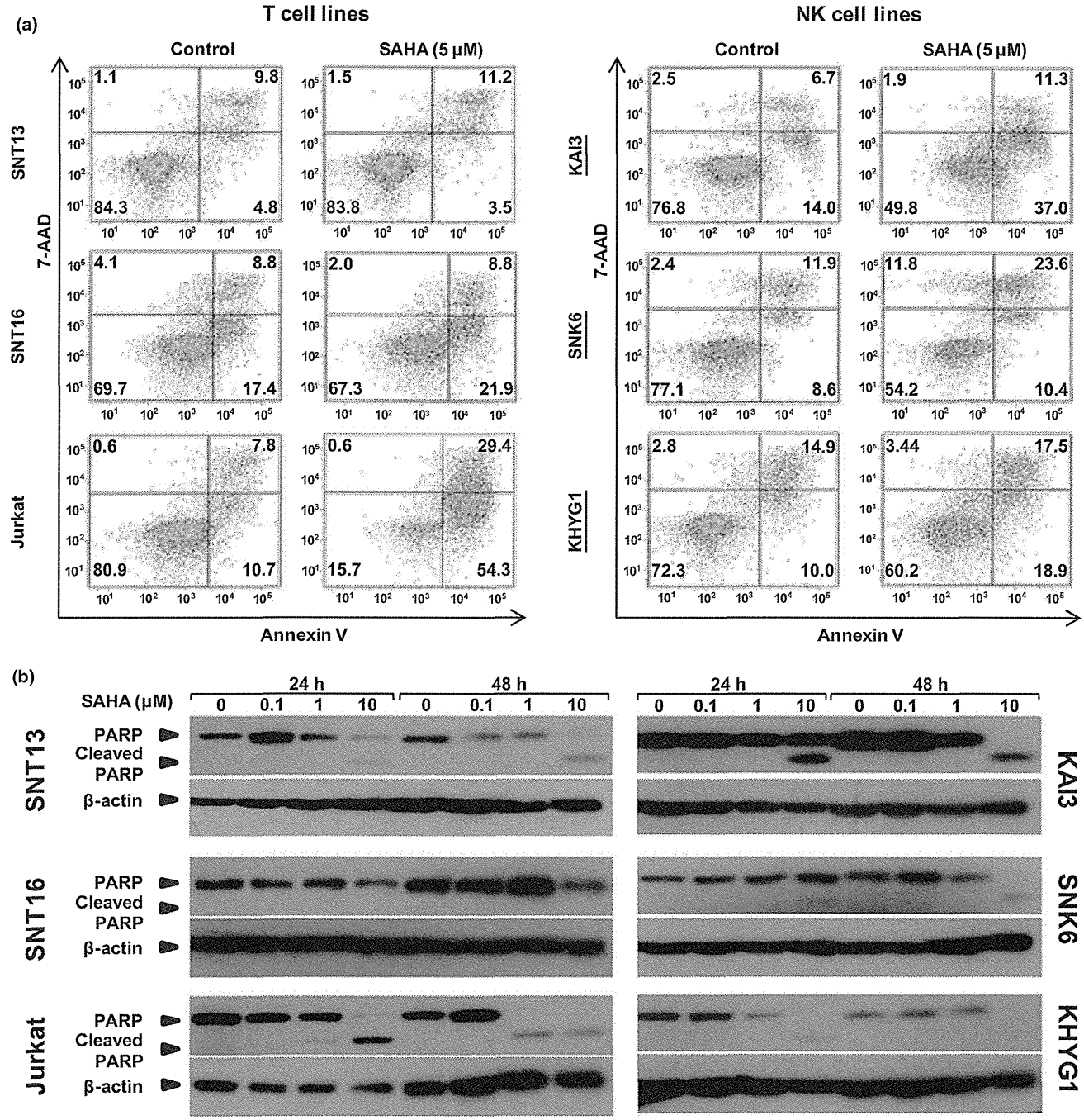

Fig. 3. Suberoylanilide hydroxamic acid (SAHA) induces apoptosis in several T and natural killer (NK) cell lines. (a) Epstein–Barr virus (EBV)-positive and EBV-negative T and NK cell lines were treated with 5 μM SAHA for 24 h. Viable cells were defined as those negative for both annexin V-PE and 7-AAD staining, and early apoptotic cells were defined as those positive for annexin V-PE but negative for 7-AAD staining. (b) T and NK cell lines were treated with the indicated concentrations of SAHA for 24 or 48 h. The cleavage of poly (ADP-ribose) polymerase (PARP) was detected by immunoblotting. β-Actin was used as a loading control.

tolerated SAHA without showing any obvious toxicity. During this period, no significant difference in the body weights of SAHA-treated and control mice was noted (data not shown). Until the end of the experiment, the size of tumors in SAHA-treated mice increased gradually, but the tumor volume was significantly less than the control group (Fig. 7a). EBER ISH showed the extent of the tumor in each mouse (Fig. 7b). In the SAHA-treated mouse, the tumor was regressed with degeneration. Additionally, SAHA-treated mice showed a significantly lower plasma EBV-DNA level (Fig. 7c). Furthermore, SAHA showed significant inhibitory effects on most EBV-encoded genes in tumor tissues (Fig. 7d). Finally, we collected samples from organs at 30 days after inoculation and performed EBER ISH. EBER-positive cells were detected in the organs of control mice, but not SAHA-treated mice (Fig. 7e). In the spleen, liver and lung, EBER-positive cells were sporadically

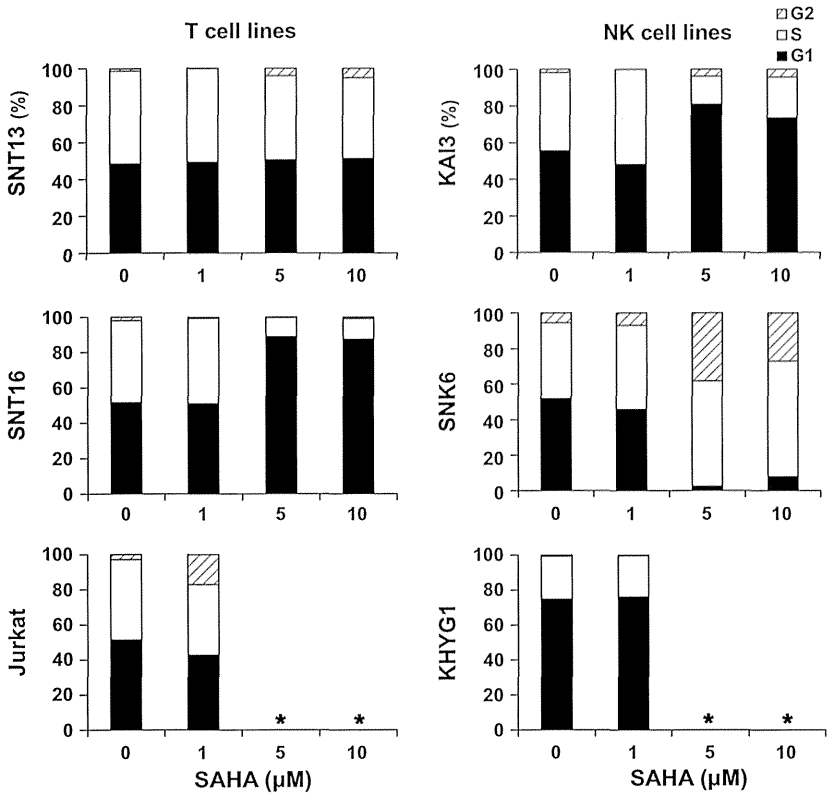

Fig. 4. Suberoylanilide hydroxamic acid (SAHA) arrests the cell cycle in T and natural killer (NK) cell lines. After treatment with the indicated concentrations of SAHA for 48 h, T and NK cell lines were fixed and stained with propidium iodide. Cell cycle profiles were assessed by flow cytometry. *Because of cell death, the cell cycle assay was indeterminable.

observed in focal lesions, indicating hematogenous dissemination of tumor cells. Conversely, the expansion of EBER-positive cells from the renal capsule to parenchyma was observed in the kidney, indicating direct invasion. These results indicated that SAHA inhibited metastasis and invasion of lymphoma cells.

Discussion

Histone deacetylase inhibitors affect tumor cell growth and survival through the induction of cell death by their characteristics of apoptosis.[6] By the upregulation of CDKNIA, HDAC inhibitors induce cell cycle arrest at the G1/S-phase. Moreover, through elongation of G2-phase, HDAC inhibitors can mediate G2/M-phase arrest, but this event occurs less frequently than G1 arrest. HDAC inhibitors can also reduce the expression of proangiogenic factors, resulting in the suppression of angiogenesis. Furthermore, HDAC inhibitors show immunomodulatory effects, which enhance tumor cell antigenicity and alter the expression of key cytokines, such as tumor necrosis factor-α, interleukin-1 and interferon-γ.[6] In the present study, SAHA markedly suppressed the proliferation of T and NK lymphoma cell lines, irrespective of the presence of EBV. The suppressive effect of SAHA was greater than that of valproic acid as demonstrated in our previous study.[8] In several T and NK cell lines, SAHA-induced apoptosis was confirmed by the increase in annexin V-positive cells and cleavage of PARP. SAHA also induced cell cycle arrest in several T and NK cell lines. The mechanism of killing appeared to differ among the cell lines. A recent study by Karube *et al.*[15] shows that suppression of the JAK-STAT pathway contributes to the suppressive effect of SAHA against NK cell lymphoma cells. Given the pleiotropic biological effects of HDAC inhibitors, it is unlikely that a single molecular pathway leading to tumor cell death will be identified in all cell types.[6]

Suberoylanilide hydroxamic acid has been reported to induce EBV lytic infection in EBV-positive gastric and nasopharyngeal carcinoma cells.[13,14] For the treatment of EBV-associated malignant diseases, induction of lytic infection is advantageous because it causes lysis of EBV-infected tumor cells. Furthermore, lytic infection should produce viral proteins with antigenicity that could induce host cellular responses. BZLF1 is an immediate-early gene and a hallmark to switch from latent gene to lytic infection.[37] In the present study, SAHA increased the expression of BZLF1 in most EBV-positive T and NK cell lines, although the late lytic gene gp350/220 was increased in only one cell line. The lytic infection induced by SAHA may play a role in its effects on EBV-infected T and NK cells. Interestingly, BZLF1, which was not expressed in the SNK-6 cell line *in vitro*, was expressed in the SNK6-derived tumor from both control and SAHA-treated mice. We speculate that the expression of BZLF1was induced in *in vivo* culture conditions presumably by nutrients or cytokines, although there is no direct poof of this.

In the present study, SAHA decreased the expression of the LMP1 gene and protein in some EBV-positive T and NK cell lines. LMP1 is a major oncoprotein that is responsible for the immortalization of primary human B lymphocytes and activation of the NF-κB, PI3K and JNK pathways.[38] Expression of LMP1 induces several pleiotropic effects, including the upregulation of adhesion molecules, anti-apoptotic proteins and cytokines. Recently, we showed that heat shock protein 90 inhibitors repress the LMP1 expression and proliferation of EBV-positive NK cell lymphoma.[35] SAHA also decreased the expression of EBNA1 in all of the cell lines. EBNA1 is essential for the maintenance of the viral episome, as well as for the initiation of latent viral replication.[38] EBNA1 also

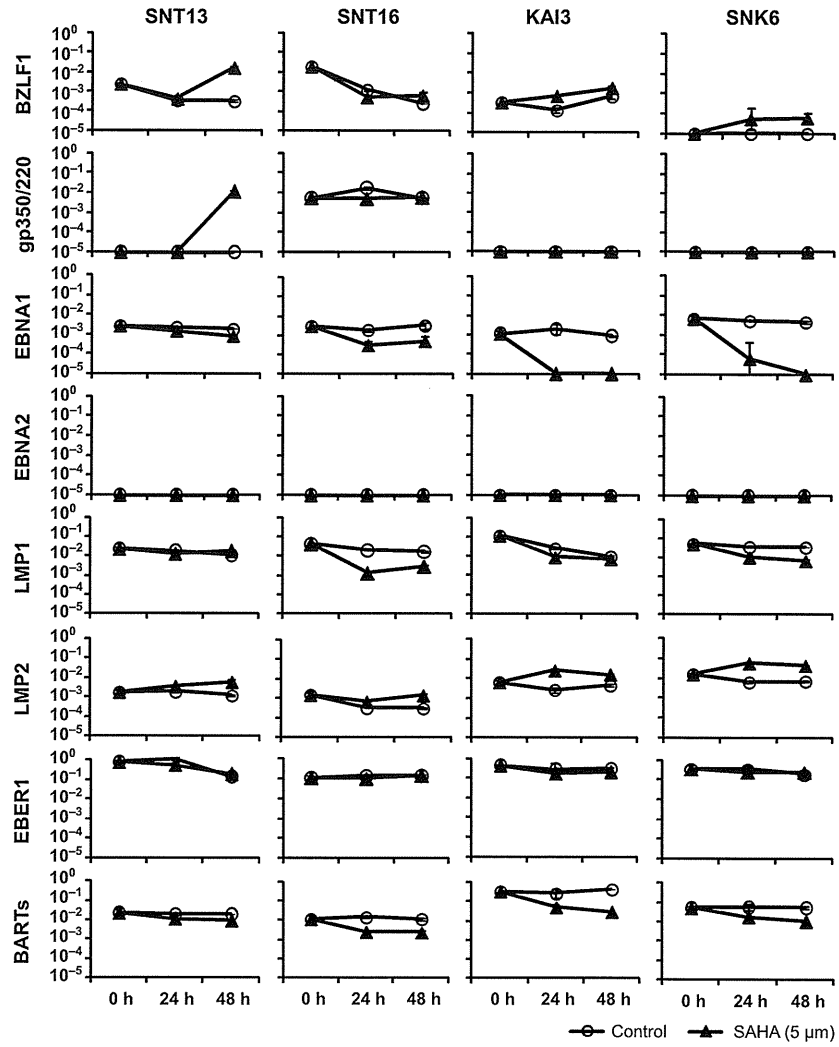

Fig. 5. Suberoylanilide hydroxamic acid (SAHA) increases the expression of Epstein–Barr virus (EBV)-lytic genes and decreases the expression of EBV-latent genes. EBV-positive T cell lines and natural killer (NK) cell lines were treated with 5 μM SAHA (closed triangles) or control (open circles) and cultured for 24 or 48 h. EBV-encoded gene expression was analyzed using real-time RT-PCR. β2-microglobulin was used as a reference gene for relative quantification, and was assigned an arbitrary value of 1 (10^0). Data are expressed as means ± SEM.

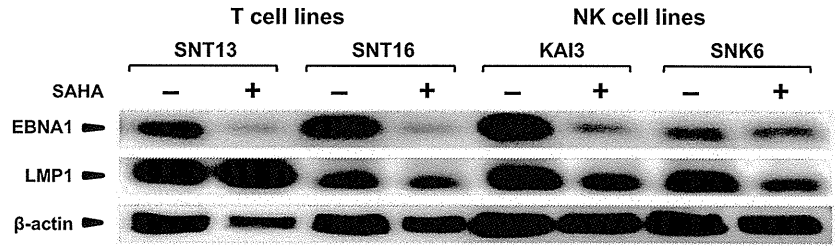

Fig. 6. Suberoylanilide hydroxamic acid (SAHA) decreases the expression of LMP1 and EBNA1 proteins in Epstein–Barr virus (EBV)-positive T and natural killer (NK) cell lines. EBV-positive T and NK cell lines were treated with 5 μM SAHA or DMSO for 48 h. EBNA1 and LMP1 were detected by immunoblotting. β-Actin was used as a loading control.

plays an important role in inhibiting apoptosis.[39] Downregulation of EBNA1 may also be associated with the suppressive effect on the proliferation of EBV-positive T and NK cell lines. Although SAHA downregulated EBV-encoded genes such as EBNA1 and LMP1, the effects of SAHA did not differ between EBV-positive and EBV-negative cell lines. The discrepancy is not clear. The EBV-positive and EBV-negative cell line sets, which were used to verify the presence/absence of EBV in the T and NK cell lines (Fig. 2a), might be inappropriate for the purpose. The EBV-positive cell lines were produced by artificial EBV infections using marker selections.[26,28] The parent cell lines can proliferate vigorously, so they did not need the help of EBV. It is also possible that the change of EBV-associated genes and proteins may be not the cause, but the result. These questions should be clarified in future studies.

We applied the murine xenograft model to further evaluate the efficacy of SAHA. Using this model, we have shown that SAHA prevented not only tumor growth but also metastasis of EBV-positive NK cell lymphoma. However, the progressive tumor growth was renewed subsequently, suggesting a limitation of single-agent therapy. Synergistic effects of HDAC inhibitors and their combination with mTOR inhibitors have been demonstrated in renal cell and prostate carcinoma cell lines.[40,41] In nasopharyngeal carcinoma, bortezomib and SAHA synergistically induced reactive oxygen species-driven caspase-dependent apoptosis and blocked the replication of EBV.[42] The combination of these agents and SAHA could

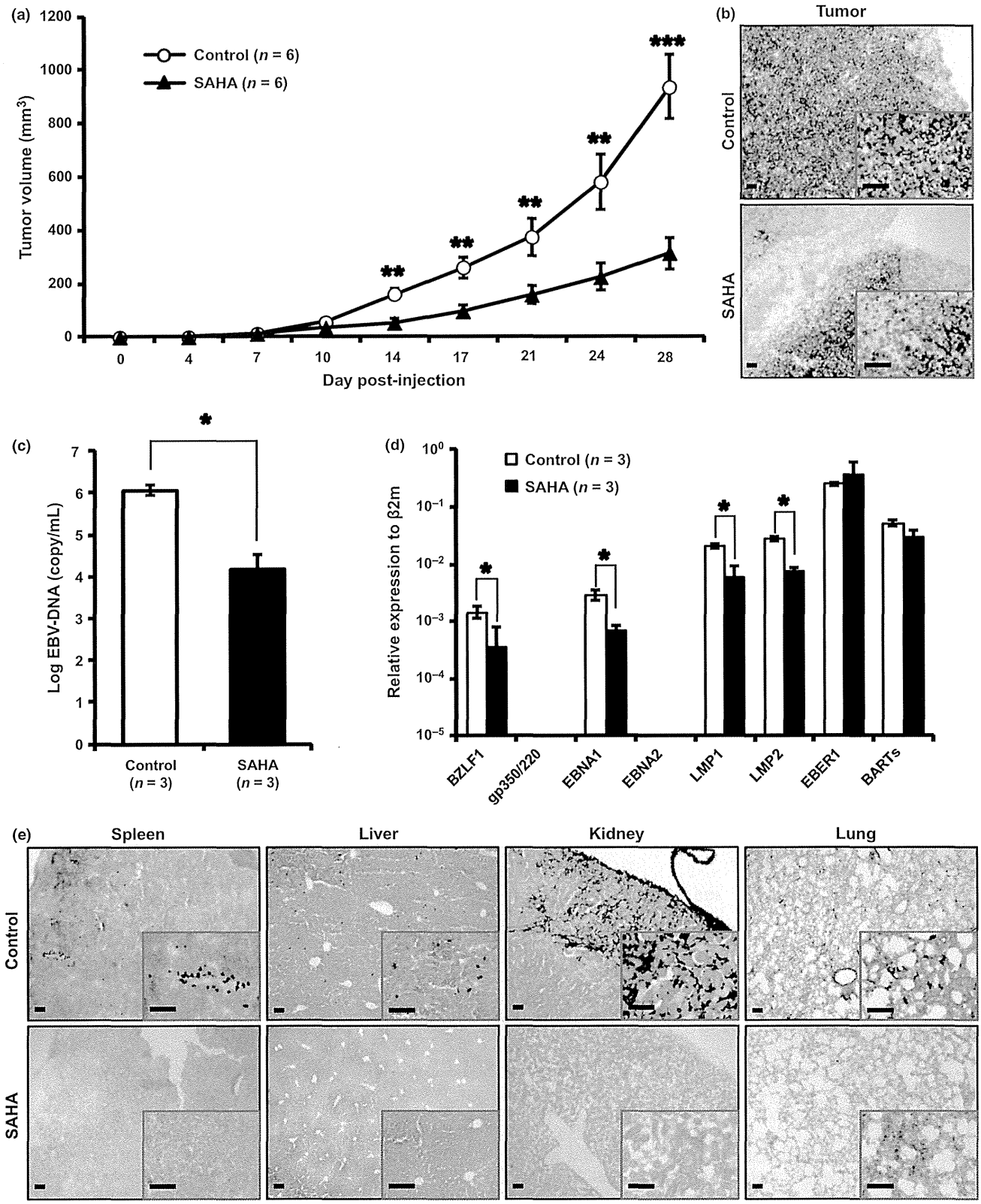

Fig. 7. Suberoylanilide hydroxamic acid (SAHA) inhibits tumor growth and metastasis of Epstein–Barr virus (EBV)-positive natural killer (NK) cell lymphoma. (a) SNK6 cells (1×10^6 per mouse) were inoculated subcutaneously into NOG mice. Mice were treated with 100 mg/kg SAHA or DMSO (control) daily from days 4 to 28. Tumor sizes were measured twice per week. (b) At 30 days after inoculation, mice were killed, and Epstein–Barr virus-encoded small RNA-positive cells were detected by *in situ* hybridization in tumor tissues of SAHA-treated or control mice (scale bars: 200 μm). (c) At 30 days after inoculation, peripheral blood was collected, and plasma was separated. EBV-DNA was quantified by real-time PCR. (d) At 30 days, EBV-related gene expression in tumor tissues was quantified. β2-Microglobulin was used for relative quantification and assigned an arbitrary value of 1 (10^0). (e) EBER-positive cells, which meant EBV-positive lymphoma cells, were detected by *in situ* hybridization in organ tissues of SAHA-treated or control mice (scale bars: 200 μm). $^*P < 0.05$, $^{**}P < 0.01$, $^{***}P < 0.002$ by Mann–Whitney *U*-test.

improve the therapy of EBV-associated T and NK cell lymphoma.

In conclusion, SAHA suppressed the proliferation of T and NK cell lines, although no significant difference was observed between EBV-positive and EBV-negative cell lines. SAHA induced apoptosis and/or cell cycle arrest in some T and NK cell lines. Furthermore, SAHA inhibited tumor progression and metastasis in a murine xenograft model. Thus, SAHA had a marked suppressive effect against EBV-associated T and NK cell lymphomas, which was mediated by either induction of apoptosis or cell cycle arrest, and could represent an alternative treatment.

Acknowledgments

The authors thank Tomoko Kunogi for technical support. We thank Norio Shimizu (Tokyo Medical and Dental University, Tokyo, Japan) and Yasushi Isobe (St. Marianna University, Kanagawa, Japan) for providing the cell lines. This study was supported by grants from the Ministry of Education, Culture, Sports, Science and Technology of Japan (25293109) and from the Ministry of Health, Labour and Welfare of Japan (H24-Nanchi-046).

Disclosure Statement

The authors have no conflict of interest.

References

1 Cohen JI. Epstein-Barr virus infection. *N Engl J Med* 2000; **343**: 481–92.
2 Williams H, Crawford DH. Epstein-Barr virus: the impact of scientific advances on clinical practice. *Blood* 2006; **107**: 862–9.
3 Suzuki R, Suzumiya J, Yamaguchi M *et al.* Prognostic factors for mature natural killer (NK) cell neoplasms: aggressive NK cell leukemia and extranodal NK cell lymphoma, nasal type. *Ann Oncol* 2010; **21**: 1032–40.
4 Cartron G, Watier H, Golay J, Solal-Celigny P. From the bench to the bedside: ways to improve rituximab efficacy. *Blood* 2004; **104**: 2635–42.
5 Heslop HE. How I treat EBV lymphoproliferation. *Blood* 2009; **114**: 4002–8.
6 Bolden JE, Peart MJ, Johnstone RW. Anticancer activities of histone deacetylase inhibitors. *Nat Rev Drug Discov* 2006; **5**: 769–84.
7 Xu WS, Parmigiani RB, Marks PA. Histone deacetylase inhibitors: molecular mechanisms of action. *Oncogene* 2007; **26**: 5541–52.
8 Iwata S, Saito T, Ito Y *et al.* Antitumor activities of valproic acid on Epstein-Barr virus-associated T and natural killer lymphoma cells. *Cancer Sci* 2012; **103**: 375–81.
9 Richon VM, Zhou X, Rifkind RA, Marks PA. Histone deacetylase inhibitors: development of suberoylanilide hydroxamic acid (SAHA) for the treatment of cancers. *Blood Cells Mol Dis* 2001; **27**: 260–4.
10 Marks PA. Discovery and development of SAHA as an anticancer agent. *Oncogene* 2007; **26**: 1351–6.
11 Stathis A, Hotte SJ, Chen EX *et al.* Phase I study of decitabine in combination with vorinostat in patients with advanced solid tumors and non-Hodgkin's lymphomas. *Clin Cancer Res* 2011; **17**: 1582–90.
12 Munster PN, Thurn KT, Thomas S *et al.* A phase II study of the histone deacetylase inhibitor vorinostat combined with tamoxifen for the treatment of patients with hormone therapy-resistant breast cancer. *Br J Cancer* 2011; **104**: 1828–35.
13 Hui KF, Chiang AK. Suberoylanilide hydroxamic acid induces viral lytic cycle in Epstein-Barr virus-positive epithelial malignancies and mediates enhanced cell death. *Int J Cancer* 2010; **126**: 2479–89.
14 Hui KF, Ho DN, Tsang CM, Middeldorp JM, Tsao GS, Chiang AK. Activation of lytic cycle of Epstein-Barr virus by suberoylanilide hydroxamic acid leads to apoptosis and tumor growth suppression of nasopharyngeal carcinoma. *Int J Cancer* 2012; **131**: 1930–40.
15 Karube K, Tsuzuki S, Yoshida N *et al.* Comprehensive gene expression profiles of NK cell neoplasms identify vorinostat as an effective drug candidate. *Cancer Lett* 2013; **333**: 47–55.
16 Ito M, Hiramatsu H, Kobayashi K *et al.* NOD/SCID/gamma(c)(null) mouse: an excellent recipient mouse model for engraftment of human cells. *Blood* 2002; **100**: 3175–82.
17 Yajima M, Imadome K, Nakagawa A *et al.* A new humanized mouse model of Epstein-Barr virus infection that reproduces persistent infection, lymphoproliferative disorder, and cell-mediated and humoral immune responses. *J Infect Dis* 2008; **198**: 673–82.
18 Shultz LD, Lyons BL, Burzenski LM *et al.* Human lymphoid and myeloid cell development in NOD/LtSz-scid IL2R gamma null mice engrafted with mobilized human hemopoietic stem cells. *J Immunol* 2005; **174**: 6477–89.
19 Sato K, Misawa N, Nie C *et al.* A novel animal model of Epstein-Barr virus-associated hemophagocytic lymphohistiocytosis in humanized mice. *Blood* 2011; **117**: 5663–73.
20 Imadome K, Yajima M, Arai A *et al.* Novel mouse xenograft models reveal a critical role of CD4+ T cells in the proliferation of EBV-infected T and NK cells. *PLoS Pathog* 2011; **7**: e1002326.
21 Zhang Y, Nagata H, Ikeuchi T *et al.* Common cytological and cytogenetic features of Epstein-Barr virus (EBV)-positive natural killer (NK) cells and cell lines derived from patients with nasal T/NK-cell lymphomas, chronic active EBV infection and hydroa vacciniforme-like eruptions. *Br J Haematol* 2003; **121**: 805–14.
22 Kaplan J, Tilton J, Peterson WD. Identification of T cell lymphoma tumor antigens on human T cell lines. *Am J Hematol* 1976; **1**: 219–23.
23 Tsuge I, Morishima T, Morita M, Kimura H, Kuzushima K, Matsuoka H. Characterization of Epstein-Barr virus (EBV)-infected natural killer (NK) cell proliferation in patients with severe mosquito allergy; establishment of an IL-2-dependent NK-like cell line. *Clin Exp Immunol* 1999; **115**: 385–92.
24 Yagita M, Huang CL, Umehara H *et al.* A novel natural killer cell line (KHYG-1) from a patient with aggressive natural killer cell leukemia carrying a p53 point mutation. *Leukemia* 2000; **14**: 922–30.
25 Miyoshi I, Kubonishi I, Yoshimoto S *et al.* Type C virus particles in a cord T-cell line derived by co-cultivating normal human cord leukocytes and human leukaemic T cells. *Nature* 1981; **294**: 770–1.
26 Fujiwara S, Ono Y. Isolation of Epstein-Barr virus-infected clones of the human T-cell line MT-2: use of recombinant viruses with a positive selection marker. *J Virol* 1995; **69**: 3900–3.
27 Robertson MJ, Cochran KJ, Cameron C, Le JM, Tantravahi R, Ritz J. Characterization of a cell line, NKL, derived from an aggressive human natural killer cell leukemia. *Exp Hematol* 1996; **24**: 406–15.
28 Isobe Y, Sugimoto K, Matsuura I, Takada K, Oshimi K. Epstein-Barr virus renders the infected natural killer cell line, NKL resistant to doxorubicin-induced apoptosis. *Br J Cancer* 2008; **99**: 1816–22.
29 Iwata S, Yano S, Ito Y *et al.* Bortezomib induces apoptosis in T lymphoma cells and natural killer lymphoma cells independent of Epstein-Barr virus infection. *Int J Cancer* 2011; **129**: 2263–73.
30 Wang D, Liebowitz D, Wang F *et al.* Epstein-Barr virus latent infection membrane protein alters the human B-lymphocyte phenotype: deletion of the amino terminus abolishes activity. *J Virol* 1988; **62**: 4173–84.
31 Daikoku T, Kudoh A, Fujita M, Sugaya Y, Isomura H, Tsurumi T. In vivo dynamics of EBNA1-oriP interaction during latent and lytic replication of Epstein-Barr virus. *J Biol Chem* 2004; **279**: 54817–25.
32 Iwata S, Wada K, Tobita S *et al.* Quantitative analysis of Epstein-Barr virus (EBV)-related gene expression in patients with chronic active EBV infection. *J Gen Virol* 2010; **91**: 42–50.
33 Kubota N, Wada K, Ito Y *et al.* One-step multiplex real-time PCR assay to analyse the latency patterns of Epstein-Barr virus infection. *J Virol Methods* 2008; **147**: 26–36.
34 Patel K, Whelan PJ, Prescott S *et al.* The use of real-time reverse transcription-PCR for prostate-specific antigen mRNA to discriminate between blood samples from healthy volunteers and from patients with metastatic prostate cancer. *Clin Cancer Res* 2004; **10**: 7511–9.
35 Murata T, Iwata S, Siddiquey MN *et al.* Heat shock protein 90 inhibitors repress latent membrane protein 1 (LMP1) expression and proliferation of Epstein-Barr virus-positive natural killer cell lymphoma. *PLoS ONE* 2013; **8**: e63566.
36 Kimura H, Morita M, Yabuta Y *et al.* Quantitative analysis of Epstein-Barr virus load by using a real-time PCR assay. *J Clin Microbiol* 1999; **37**: 132–6.
37 Longnecker RM, Kieff E, Cohen JI. Epstein-Barr virus. In: Knipe DM, Howley PM, eds. *Fields Virology*, 6th edn. Philadelphia: Wolters kluwer/Lippincott Williams & Wilkins, 2013; 1898–959.
38 Damania B. Oncogenic gamma-herpesviruses: comparison of viral proteins involved in tumorigenesis. *Nat Rev Microbiol* 2004; **2**: 656–68.
39 Saridakis V, Sheng Y, Sarkari F *et al.* Structure of the p53 binding domain of HAUSP/USP7 bound to Epstein-Barr nuclear antigen 1 implications for EBV-mediated immortalization. *Mol Cell* 2005; **18**: 25–36.
40 Mahalingam D, Medina EC, Esquivel JA *et al.* Vorinostat enhances the activity of temsirolimus in renal cell carcinoma through suppression of survivin levels. *Clin Cancer Res* 2010; **16**: 141–53.

41 Thelen P, Krahn L, Bremmer F, Strauss A, Brehm R, Loertzer H. Synergistic effects of histone deacetylase inhibitor in combination with mTOR inhibitor in the treatment of prostate carcinoma. *Int J Mol Med* 2013; **31**: 339–46.

42 Hui KF, Lam BH, Ho DN, Tsao SW, Chiang AK. Bortezomib and SAHA synergistically induce ROS-driven caspase-dependent apoptosis of nasopharyngeal carcinoma and block replication of Epstein-Barr virus. *Mol Cancer Ther* 2013; **12**: 747–58.

Supporting Information

Additional supporting information may be found in the online version of this article:

Fig. S1. SNK6 is less dependent of human interleukin-2 (IL-2) compared with other Epstein–Barr virus (EBV)-positive T and natural killer (NK) cell lines.

Table S1. Engraftment of cell lines into NOG mice.